Materials Horizons

REVIEW

Cite this: *Mater. Horiz.*, 2024, **11**, 5181

An evaluation of recent advancements in biological sensory organ-inspired neuromorphically tuned biomimetic devices

Animesh Sinha,[a] Jihun Lee,[a] Junho Kim [a] and Hongyun So *[ab]

In the field of neuroscience, significant progress has been made regarding how the brain processes information. Unlike computer processors, the brain comprises neurons and synapses instead of memory blocks and transistors. Despite advancements in artificial neural networks, a complete understanding concerning brain functions remains elusive. For example, to achieve more accurate neuron replication, we must better understand signal transmission during synaptic processes, neural network tunability, and the creation of nanodevices featuring neurons and synapses. This study discusses the latest algorithms utilized in neuromorphic systems, the production of synaptic devices, differences between single and multisensory gadgets, recent advances in multisensory devices, and the promising research opportunities available in this field. We also explored the ability of an artificial synaptic device to mimic biological neural systems across diverse applications. Despite existing challenges, neuroscience-based computing technology holds promise for attracting scientists seeking to enhance solutions and augment the capabilities of neuromorphic devices, thereby fostering future breakthroughs in algorithms and the widespread application of cutting-edge technologies.

Received 1st May 2024,
Accepted 18th July 2024

DOI: 10.1039/d4mh00522h

rsc.li/materials-horizons

Wider impact

This study provides a comprehensive analysis of algorithms designed to mimic the operational characteristics of the human brain. Furthermore, we discuss the sensory systems and constraints inherent in newly built single- and multisensory devices. The subsequent section explores prevailing research patterns in neuromorphically-tuned devices. Neuromorphic engineering refers to the advancement of systems that imitate the functioning of the human brain to achieve enhanced energy efficiency, parallelism, and cognitive capabilities for numerous activities, including, but not limited to, object identification, association, adaptability, and learning. Neuromorphic devices have significant potential as innovative computer architectures that provide energy-efficient devices with excellent precision. Here, we discuss the prevalent issues identified by various authors and identify potential areas for improvement that directly influence the advancement of AI-integrated gadgets. This review also seeks to unveil the advancements in neuroscience, enabling a comprehensive exploration of the capabilities and practical applications of neuromorphic science.

[a] *Department of Mechanical Convergence Engineering, Hanyang University, Seoul 04763, South Korea. E-mail: hyso@hanyang.ac.kr*
[b] *Institute of Nano Science and Technology, Hanyang University, Seoul 04763, South Korea*

Animesh Sinha

Animesh Sinha received his M.S. from the National Institute of Technology Silchar, India, in 2015 in the specialization of Materials and Manufacturing Technology. Later he worked as an Assistant Professor from 2015–2021. He is currently doing his PhD at Hanyang University, South Korea, under Global Korea Scholarship. His research interests include the synthesis of nanomaterials, sensors, semiconductors, energy storage devices, etc.

Jihun Lee

Jihun Lee received his BS and MS degrees from the Mechanical Convergence Engineering department at Hanyang University, South Korea, under Prof. Hongyun So. He is currently pursuing his PhD at the University of Michigan, Ann Arbor. His research interests include biomedical devices, micromachining, sensors, and actuators.

1. Introduction

Since 2010, mortality rates of neurological diseases have been on the rise.[1] Neurological conditions have emerged as the leading cause of impairment in humans, accounting for approximately 9 million deaths annually.[2] Consequently, effective management of neurological illnesses necessitates specialized treatment, encompassing access to medical specialists, a variety of diagnostic tools, and intricate therapeutic modalities. Unfortunately, in most real-life situations, there exists a shortage of resources, leading to inadequate provision of treatment for individuals with neurological disorders.[3] Furthermore, the complex nature of these conditions poses challenges in accurate diagnosis and treatment, often resulting in misdiagnosis and delayed medical intervention. Addressing these challenges requires a comprehensive understanding of the brain, entailing its brain functions and underlying mechanisms.[4,5] Among recently developed advanced artificial intelligence (AI)-driven electronic breakthroughs, neuromorphic computing stands out as the most attractive and innovative technology.[6–12] The term "neuromorphic" is derived from "neuro," referring to the nervous system, and "morphic," indicating shape or form. A neuromorphic system is a computational system that replicates the architecture and behavior of the human brain.[13] For easy understanding, neuromorphic computing involves engineering advancements aimed at replicating the operations of the human brain to achieve optimal energy consumption, processing speed, and cognitive skills, such as object recognition, associative thinking, adaptation, and learning.

While neuromorphic systems strive to mimic brain functionality for executing basic machine-learning tasks, their primary benefit lies in the utilization of analog and mixed-signal versions of essential perceptron networks and complex spiking neural networks. Synapses in the brain allow neurons to process information and create memories.[14] This design enables the brain to quickly and efficiently perform complex calculations, with minimal energy consumption. In recent years, significant developments have been made in neuromorphic systems, including organic electrochemical neuromorphic devices,[15–20] neuromorphic memristors,[21–25] stretchable neuromorphic efferent nerves,[26–28] synaptic devices,[29–35] neuromorphic chips,[36–39] and robots,[40–43] among others. Although neuromorphic systems hold promise for the future, they require further development to demonstrate their efficacy as tools for neuroscience research. This underscores the difficulties faced by the neuromorphic community. Despite the inherent structural advantages of neuromorphic systems, researchers must compete with the well-established products of traditional computing that have undergone generations of optimization and have been meticulously tailored to the underlying manufacturing technology.

The human brain comprises billions of neurons linked by trillions of synapses.[11] Consequently, scientists worldwide are actively exploring optimal material combinations for creating artificial synapses capable of handling massive amounts of complex data in realistic environments while consuming minimal power.[44] Moreover, artificial synaptic devices face challenges such as rapid information transmission, susceptibility to spikes, and the need for large-scale integration, necessitating significant research focus.[45] Hardware computer systems draw inspiration from the brain's hierarchical organization, with the neurosynaptic architecture powering these artificial neural networks through transistors.[46] In massive computer systems, billions of transistors are integrated into a single silicon chip.[47] Furthermore, several significant distinctions exist between the computing principles of the brain and silicon-based computers. First, computers segregate processing and storage units, whereas the brain integrates neurons and synapses in close proximity. Second, the extensive three-dimensional (3D) connectivity of the brain surpasses the capabilities of silicon technology, which can only support connections in two dimensions.[11,48] Computer transistors function primarily as switches to create deterministic Boolean circuits, while spike-based event-driven computations in the brain are inherently stochastic.[49] Additionally, these additional factors must be evaluated. First, evaluating the feasibility of implementing increasingly complex algorithms on an implanted device is essential. Second,

Junho Kim

Junho Kim received his BS degree from Hanyang University, South Korea. He is currently pursuing a combined MS/PhD degree at Hanyang University, under the supervision of Prof. Hongyun So, in the Mechanical Convergence Engineering Department. His research interests include biomedical devices, energy harvesting, sensors, and actuators.

Hongyun So

Hongyun So received the PhD degree from the University of California at Berkeley in 2014 in Mechanical Engineering. He joined Stanford University in 2015 as a Post-Doctoral Scholar with the Aeronautics and Astronautics Department. He is currently an Associate Professor with the Mechanical Engineering Department and Deputy Director of Advanced Semiconductor Packaging Center, Hanyang University. His research interests include design, modeling, and manufacturing of micro/nanosystems, harsh-environment sensors, advanced semiconductor packaging, and mechanical issues related to heat transfer and fluid mechanics.

determining how these algorithms can effectively adapt to patient preferences is necessary. Stacey highlighted the use of deep learning in neuromorphic chips that operate with limited power and demonstrate significant predictive capabilities for detecting seizures with easy tunability.[50] Similarly, Isabell *et al.* investigated the viability of a customizable system for predicting epileptic seizures using a low-energy neuromorphic device.[51]

Complementary metal-oxide semiconductor (CMOS) technology is the most advanced technology implemented thus far in the field of neuromorphic engineering.[8,52] This method effectively reduces power consumption during neuromorphic computations. However, CMOS technology suffers from data storage limitations as it loses all data during power failure. Currently, researchers are shifting their focus towards leveraging nonvolatile random-access memory (NVRAM).[53,54] With the emergence of NVRAM devices, circuit designers can now explore avenues to enhance the energy efficiency of core deep neural network (DNN) operations. These devices offer advantages such as low switching energy, high density, and superior durability compared to conventional devices. However, due to the unknown precise number of neurons interacting within the brain to produce intricate cognitive processes, replicating the brain's neural network and data storage remains challenging. The demand for analog designs has expanded to include mixed-signal designs, resulting in the development of various advanced analog and digital semiconductor circuits.

Individuals are frequently exposed to stimuli that engage multiple senses, including visual perception, hearing sensation, haptic sensation, gustation, and olfaction. A singular sensory system that measures a single stimulus often requires a high estimation accuracy rate. Signals from various sources are often noisy and unreliable.[55,56] Developing techniques to reduce noise and fluctuations, while preserving computational efficiency, is crucial for real-world applications. Therefore, there is a need for devices with faster signal processing capabilities. Alternatively, integrating multiple sensory modalities may enhance object localization and precision detection.[57,58] Humans naturally rely on multiple sensory modalities that bear considerable resemblance to multimodal brain networks.

This review aims to provide a comprehensive understanding of artificial neurons and their essential functions in biomimetic applications. The topic is currently undergoing intensive research, primarily involving numerical analysis based on a few hardware applications. While neuromorphically-tuned devices boast diverse applications, it is challenging to encompass them all within a single study. Nonetheless, we have endeavored to review all recently developed neuromorphically-tuned biomimetic devices, elucidating their fabrication processes and applications. In Section 2, we delve into the inspiration behind artificial synapse systems, while Section 3 explores the currently used materials, such as organic, inorganic, organic–inorganic hybrids, and perovskite quantum dots (PQDs) for fabricating devices. We also compared single and multisensory systems, spike-based memristors, artificial vision systems, UV light detection, and color recognition. Section 5 describes butterfly- and spiderweb-inspired neuromorphic devices. Fig. 1 presents the most commonly used algorithms, as well as recently used materials for

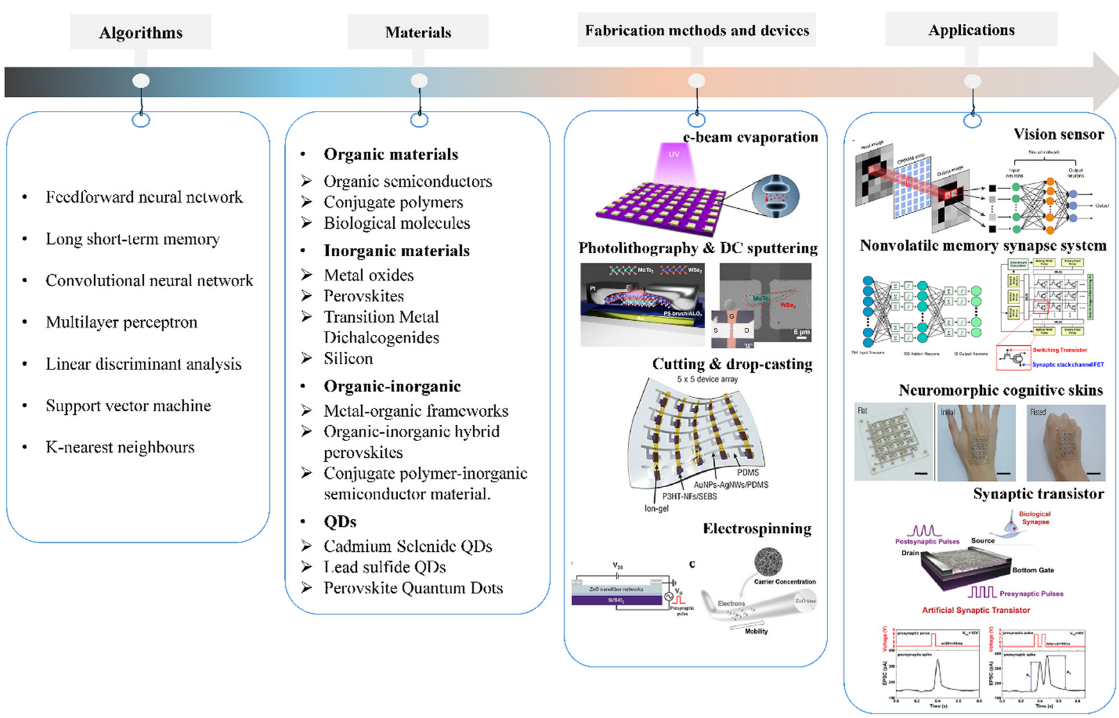

Fig. 1 Overall depiction of algorithms, materials utilized, fabrication techniques and gadgets, and applications of neuromorphically tuned biomimetic devices. Reproduced with permission from ref. 59. Copyright 2019, Nature Publishing Group. Reproduced with permission from ref. 60. Copyright 2020, American Chemical Society. Reproduced with permission from ref. 61. Copyright 2022, The National Academy of Sciences. Reproduced with permission from ref. 62. Copyright 2023, Wiley-VCH.

device fabrication and their respective applications. Finally, we highlight the current research gaps and the extensive potential of this subject, proposing new research paths to address real-world challenges. These endeavors will facilitate the development of more effective devices, enhancing existing neural network systems and fostering progress across several fields, such as robotics, sensory technologies, and healthcare monitoring.

2. Synapse systems

The term "synapse" was introduced by Sir Charles Sherrington in 1897 to denote the point of connection between nerve cells.[63] Synapses represent physically recognizable cellular sites where functional connections occur between neurons. Neuronal communication is essential for brain activity, as its effectiveness allows pre-established neural networks to operate dynamically.[64]

2.1. Biological synaptic systems

Axons predominantly establish synapses in the brain, often organizing them linearly, resembling pearls on a string. When a single presynaptic neuron forms numerous connections to a postsynaptic cell, it reduces transmission failures but restricts the possibility of synaptic transformation (Fig. 2A). Presynaptic neurons release neurotransmitters, while postsynaptic neurons detect these neurotransmitters using various receptors (including glutamate receptors, glycine receptors, and protein receptors).[65] All receptors have unique functions in the synaptic system. For instance, glutamate receptors play a crucial role in facilitating excitatory communication between neurons in the brain. They are particularly important in processes such as memory formation, learning, and neurodegenerative conditions.[66] Glycine receptors are crucial for enabling rapid inhibitory communication between the nerve cells in the spinal cord and brainstem.[67] G protein-coupled receptors, in contrast, are transmembrane protein molecules with similar structures that enable the nervous system to react correctly to external stimuli and internal conditions.[68]

The burgeoning efforts in AI have been considerably influenced by the biological realm, where people and animals interact with each other to enhance the effectiveness of regular activities. This ongoing two-way interaction between organisms has contributed to continuous improvements in abilities, knowledge, and complexity. Consequently, biomimetic artificial synaptic systems with diverse structures and operational mechanisms have been developed as a result.

2.2. Artificial synaptic systems

The development of artificial synapses that mimic biological synaptic functions and can be seamlessly integrated into computing systems is crucial for advancing human life. These systems should exhibit characteristics such as high compactness, multipurpose functionality, autonomous learning capabilities, adaptability to new circumstances, sustainability, and the ability to simultaneously store and analyze data. However, limitations in materials science (including delays in developing new materials, understanding material properties, environmental impact, and efficiency) currently impede the progress of neuromorphic systems and gadgets linked to AI. Researchers have explored various artificial synaptic systems, such as chemical synapses,[64,70–72] electrical synapses,[73–77] electrochemical synapses,[46,78–81] and photonic synapses[82–86] (Fig. 2B).

In chemical synapses, communication occurs *via* the secretion of a neurotransmitter from a specific neuron and its recognition by a neighboring cell.[86] Here, chemical transmission relies on complex presynaptic molecular systems that control the release of neurotransmitters in a probabilistic manner (Fig. 2C), necessitating an intricate postsynaptic system.[87] Conversely, electrical synapses involve the direct connection of the cytoplasm of

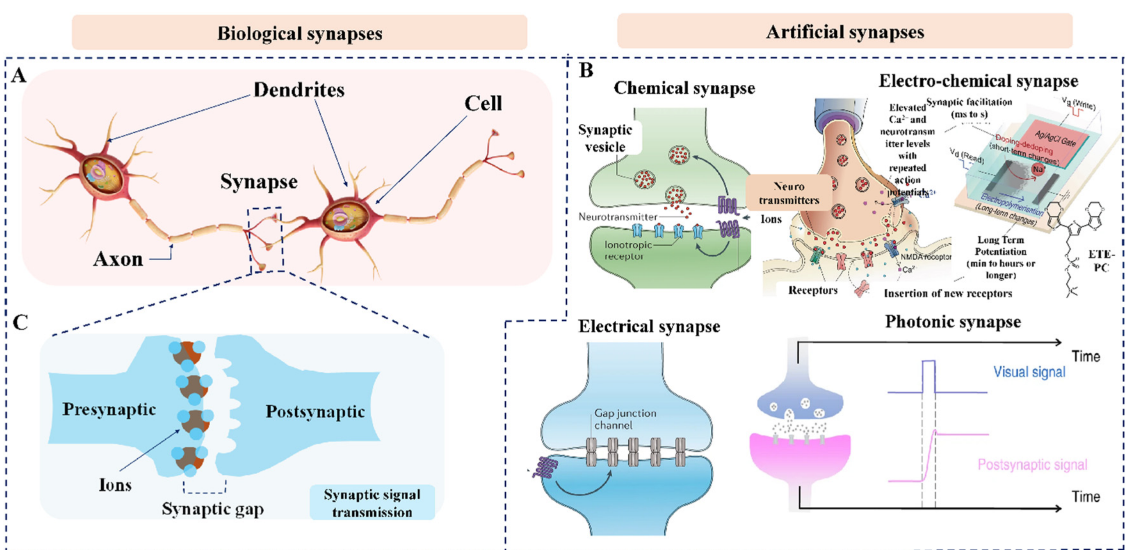

Fig. 2 (A) Illustration of a biological synaptic system. (B) Various types of artificial synaptic systems: chemical, electrical, electro-chemical, and photonic. Reproduced with permission from ref. 64. Copyright 2014, Nature Publishing Group. Reproduced with permission from ref. 46. Copyright 2022, (CC BY 4.0) Nature Publishing Group. Reproduced with permission from ref. 69. Copyright 2022, (CC BY 4.0) Nature Publishing Group. (C) Represents synaptic signal transmission.

neighboring cells through the clustering of intercellular channels known as gap junctions. These gap junctions directly link the interiors of two adjacent cells.[88] Furthermore, electrochemical measurements of neurotransmitters have conventionally been used to assess their transportation beyond synapses, providing valuable insights into the relationship between neural communication and behavior.[89]

Some researchers have explored the use of electrochemical synapse systems to develop various devices, such as protonic synapses for solid-state devices,[88] non-volatile organic electrochemical devices (NVOECDs),[15] organic electrochemical transistors (OECTs),[79,90] and organic electrochemical synaptic devices (OECSDs)[78]. Additionally, Huang *et al.* and Chen *et al.* provided comprehensive analyses of the processes and practical applications of chemical synaptic systems.[91,92] Harikesh *et al.* compared biological synapses and printed organic electrochemical synapses (OECSs) to demonstrate the learning behavior and effectiveness of their system. They indicated that the switching characteristics of the transistor, which depend on ionic concentration, can effectively modulate the spiking frequency.[46] This modulation closely resembles the behavior of biological systems and has potential applications in event-based sensors. According to Bhunia *et al.*, OECTs offer excellent sensitivity, operational stability, and low electrical consumption.[93] Despite these several advantages, it is imperative to concurrently address the following key aspects, which are essential for ensuring a robust fabrication process of electrochemical synaptic devices:

(1) Understanding the process of ion penetration through a dielectric barrier into a semiconductor layer is crucial for the development of artificial synaptic networks.[94]

(2) It is essential to comprehend the impact of various characteristics of transistor devices, including their microscopic structure, population density, and material interface.[95]

(3) The transformation of theoretical modeling into practical artificial synapses necessitates a deep understanding of complex chemical dynamics.

Recently, photonic synaptic devices have gained increasing popularity due to their distinct advantages over electronic synaptic devices, including broad bandwidth, reduced crosstalk, and low power consumption capabilities.[96–100]

Artificial photonic synaptic components, capable of both detecting light and facilitating synaptic transmission in a single device, are emerging as strong contenders among existing photonic synapses. These devices react directly to external light stimuli, enabling temporary memory and instantaneous analysis of optical data and information. Hence, photonic synapses not only perceive light signals but also record the entire chronology of events, encompassing light intensity and the quantity, length, and frequency of light spikes, effectively simulating the retina's sense of sight. Moreover, photonic synaptic devices offer a broader bandwidth, superior resistance to interference, and reduced crosstalk compared to electronic synapses.[100,101] In a recent study, Wang *et al.* investigated the development of artificial neural systems (particularly, neuromorphic vision sensors) leveraging the concept of biological visual systems.[102] They analyzed the fundamental components of the human eye, such as the retina, optic nerves, and brain, and their collaborative functionality (Fig. 3A). These components transform the external optical inputs into electrical impulses, which are then converted into ionic signals. Synapses analyze, interpret, and store these signals, with the retina preprocessing these signals before sending them to the primary visual cortex for recognition and information processing. However, when the top electrode of a 2T vertical photodetector (Fig. 3B) is positively biased, it generates an external electric field that flows from the top to the bottom. Each electrical stimulation causes the iodine vacancies to move up and down through the inorganic layers. This action causes negatively charged ions to move in the opposite direction. Nevertheless, the significant presence of BA^+ hinders the migration of I^-, leading to increased barriers for ion migration. Consequently, vacancies with a positive charge migrate towards higher inorganic material layers, while negative ions accumulate at the bottom. The authors proposed that implementing enhanced repeated training of an artificial synaptic system could achieve a commendable recognition rate of 94.01%.

However, the utilization of these techniques may exacerbate the complexity of the manufacturing procedure and the increase the energy consumption of the gadget, necessitating a controlled process environment. Kim *et al.* fabricated a photonic synaptic device using an oxide semiconductor and a ferroelectric material, enabling tunable synaptic functions through a ferroelectric layer. Similarly, other researchers have developed gate-tunable $InGaZnO_4$ semiconductors,[103] tunable synaptic transistors,[104] tunable ionic electrolyte transistors,[105] and tunable opto-synaptic devices,[106] highlighting the potential of photonic synapses in neuromorphic device applications.

3. Fabrication of artificial synaptic devices

3.1. Inorganic-based devices

Replicating energy-efficient brain function on a single device is a challenging task. However, the energy-saving potential of these methods is restricted by the significantly higher power consumption of computer systems tasked with simulating the complexity of the human brain. The inefficiency of conventional systems stems largely from the architectural design known as the von Neumann system,[107] which creates a bottleneck that requires constant storage and extraction of information from various system components, rendering it one of the least energy-efficient methods. Some researchers have explored a hardware-based approach using silicon neuron (SiN) as an energy-efficient device (Fig. 4A),[108,109] CMOS for spike neuron memristors (to better mimic biological synapses and multimodal sensing) (Fig. 4B),[110] and halide perovskite film ($CsCu_2I_3$) (as an eco-friendly, highly stable device (Fig. 4C)).[111] Halide perovskites exhibit superior hysteresis compared to other materials due to their low activation energy for ion migration, alongside their rapid switching rate.[112] This can be attributed to the intricate interplay between metal and halide ions. However, their thermal instability and hygroscopicity have led researchers to seek substitutes for certain types of halide perovskites, such as organometallic halide perovskites.[113,114] These characteristics may also

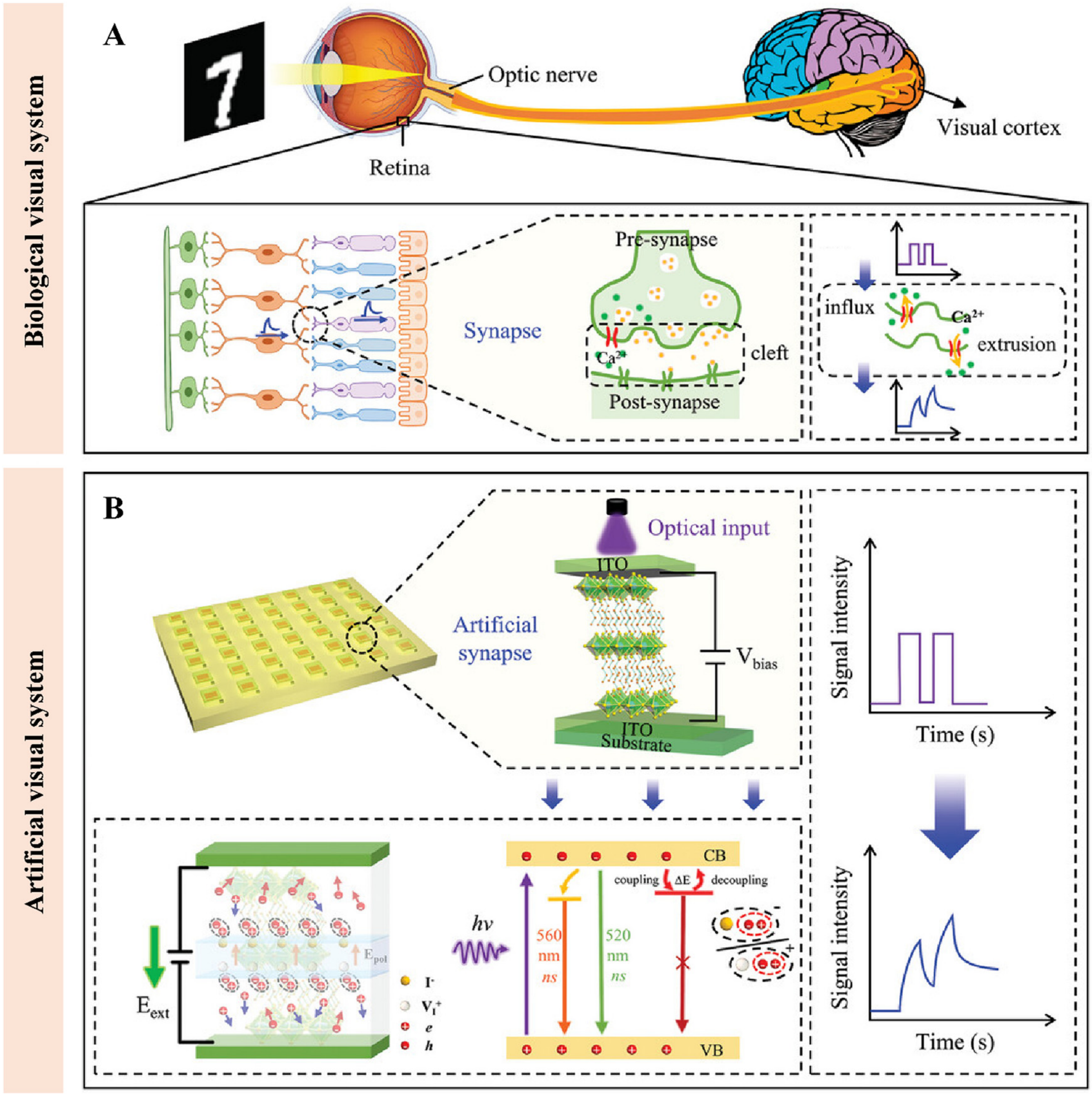

Fig. 3 (A) Biological vision system, including optic nerves with a visual cortex explaining the multilayer structure of the retina. (B) 2T vertical photodetector inspired by a biological retinal system. Reproduced with permission from ref. 102. Copyright 2024, Wiley-VCH.

indirectly render them vulnerable to environmental factors (such as water or water molecules). Lead-halide perovskites have garnered attention for their excellent power-conversion efficiency and potential for low-temperature fabrication.[115–117] We recommend that researchers refer to the literature published by Vats *et al.* for a deeper understanding of functional neuromorphic devices fabricated from metal halide perovskites.[118]

Nonetheless, neuromorphic devices fabricated using inorganic materials are delicate and are unsuitable for flexible and adaptable applications. Furthermore, these materials lack the necessary biocompatibility or biodegradability required for implantable applications or for the production of dependable synaptic devices.

3.2. Organic-based devices

Biological detection systems serve two primary functions: detection and adaptation.[119] These systems enhance responses to external stimuli and adapt to continuous background inputs. Bioelectronic sensors utilize biological sensing receptors to identify specific molecules or chemical analytes and generate electrical signals. Conversely, artificial sensory mechanisms may convert an external input into an electrical signal, and then modulate the electrical impulse into either an excitatory or inhibitory current or potential.[120] Organic materials are preferred for neuromorphic device fabrication due to their suitability for large-scale production and their biocompatible properties.[121]

Organic material-based electronics closely mimic biological substitutes and exhibit both short- and long-term plasticity.[122,123] The hardware implementation of artificial neural networks typically follows a top-down approach based on conventional technology, requiring proficiency in network structures. In contrast, biology primarily functions through a bottom-up approach. However, organic material-based electronics face issues such as the need for larger memory capacity

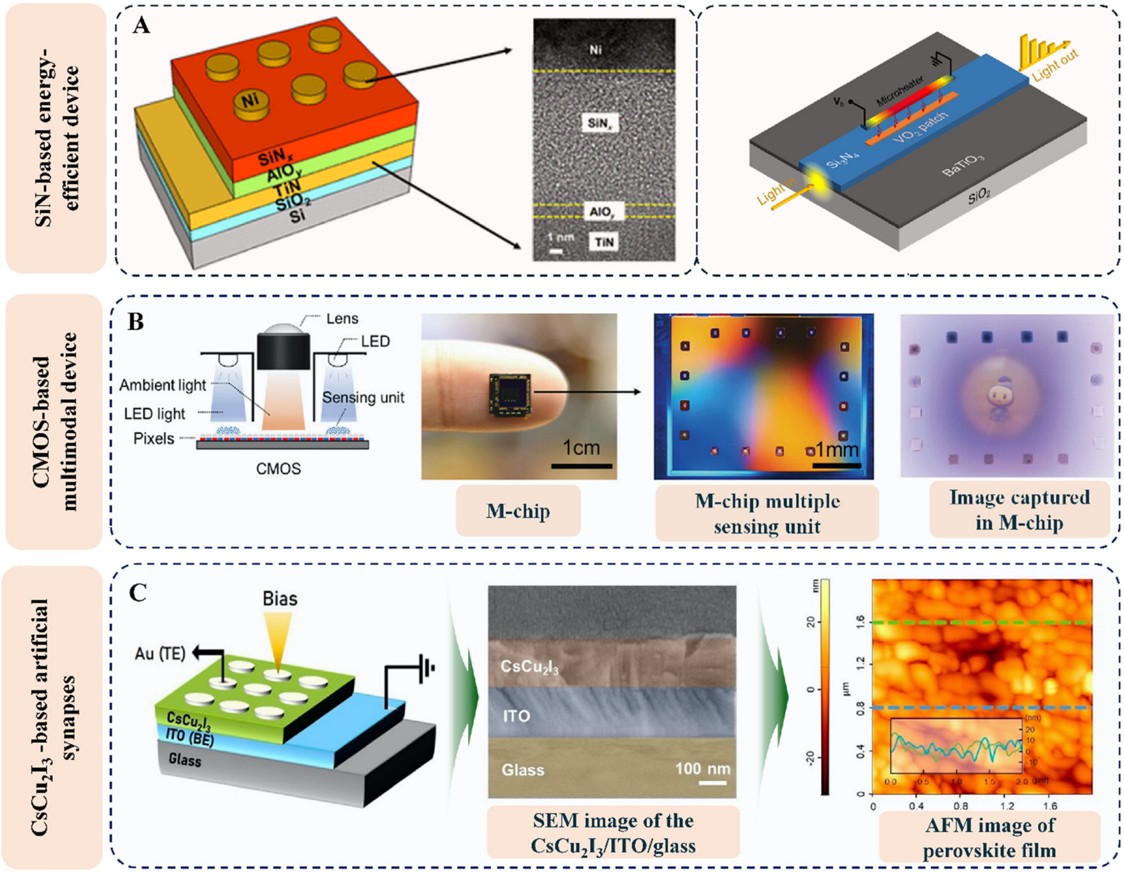

Fig. 4 (A) Silicon nitride memristor with the TEM micrograph (left side). Hybrid barium titanite ($BaTiO_3$)/silicon nitride (SiN) photonic platform (right side). Reproduced with permission from ref. 108. Copyright 2017, American Chemical Society. Reproduced with permission from ref. 109. Copyright 2023, Optica publishing group. (B) CMOS imager chip. Reproduced with permission from ref. 110. Copyright 2023, Wiley-VCH. (C) Schematic representation of synaptic device fabricated by $CsCu_2I_3$ perovskite thin film with cross-sectional scanning electron microscopy (SEM) and atomic force microscopy (AFM) micrograph image. Reproduced with permission from ref. 111. Copyright 2022, American Chemical Society.

and higher energy consumption when compared to inorganic material-based systems. Janzakova *et al.* developed a novel organic material device composed of dendritic PEDOT:PSS fibers using a bottom-up approach to enhance computing performance (Fig. 5A).[124] Their findings provide insight into high-potential algorithmic improvements using structural plasticity learning and minimizing screening requirements required for a wide range of random topologies. Nevertheless, the authors could consider including additional recommendations for techniques to reduce the number of training phases.

Numerous studies have been conducted to develop energy-efficient artificial synaptic devices using organic materials. For example, in 2016, Xu *et al.* devised a synaptic transistor utilizing organic nanowires to minimize energy consumption.[126] In 2017, Burgt *et al.* presented a 3D design that closely resembled the human brain, alongside an electrochemical neuromorphic organic system that demonstrated efficiency in terms of energy use and expenses.[15] In addition, Tanim *et al.* established an artificial synaptic device using a blend of honey and CNT.[127] However, certain constraints remain, such as the development of an effective, biodegradable, and wearable synaptic transmitter. Oh *et al.* recently produced a PVA-based memristor (Fig. 5B) that enhanced synaptic plasticity and reduced energy use.[125] The author used parallel computation (Fig. 5C) to assess the potential of the PVA-based memristor for building sophisticated neural networks. They trained the memristor using the logic operators OR and AND (Fig. 5D) and evaluated the amount of energy utilized during training. Researchers assessed the dependability of the memristor using two binary inputs (V_1 and V_2) and confirmed it by measuring the output currents (I_{OR} and I_{AND}) (Fig. 5E). Fig. 5F shows the SPICE numerical simulation results for handwritten digit pattern recognition. A flexible memristor links the input and output neurons, as illustrated in Fig. 5G. After 50 epochs, the learning procedures translated the ideal weight distribution (Fig. 5H) into the cell conductance in the device arrays, as well as the memristor array conductance distribution (Fig. 5I). After 50 epochs of training, the neural network achieved a pattern recognition accuracy of 92% on the constructed memristor (Fig. 5J), approaching the efficiency of an ideal software system that reflects the efficiency of the device.

However, there are still concerns to address, such as attaining multidimensional conductance, regulated isotropic charge transfer, comprehending the training model, and achieving intrinsic material features, such as molecular packing. Considering these

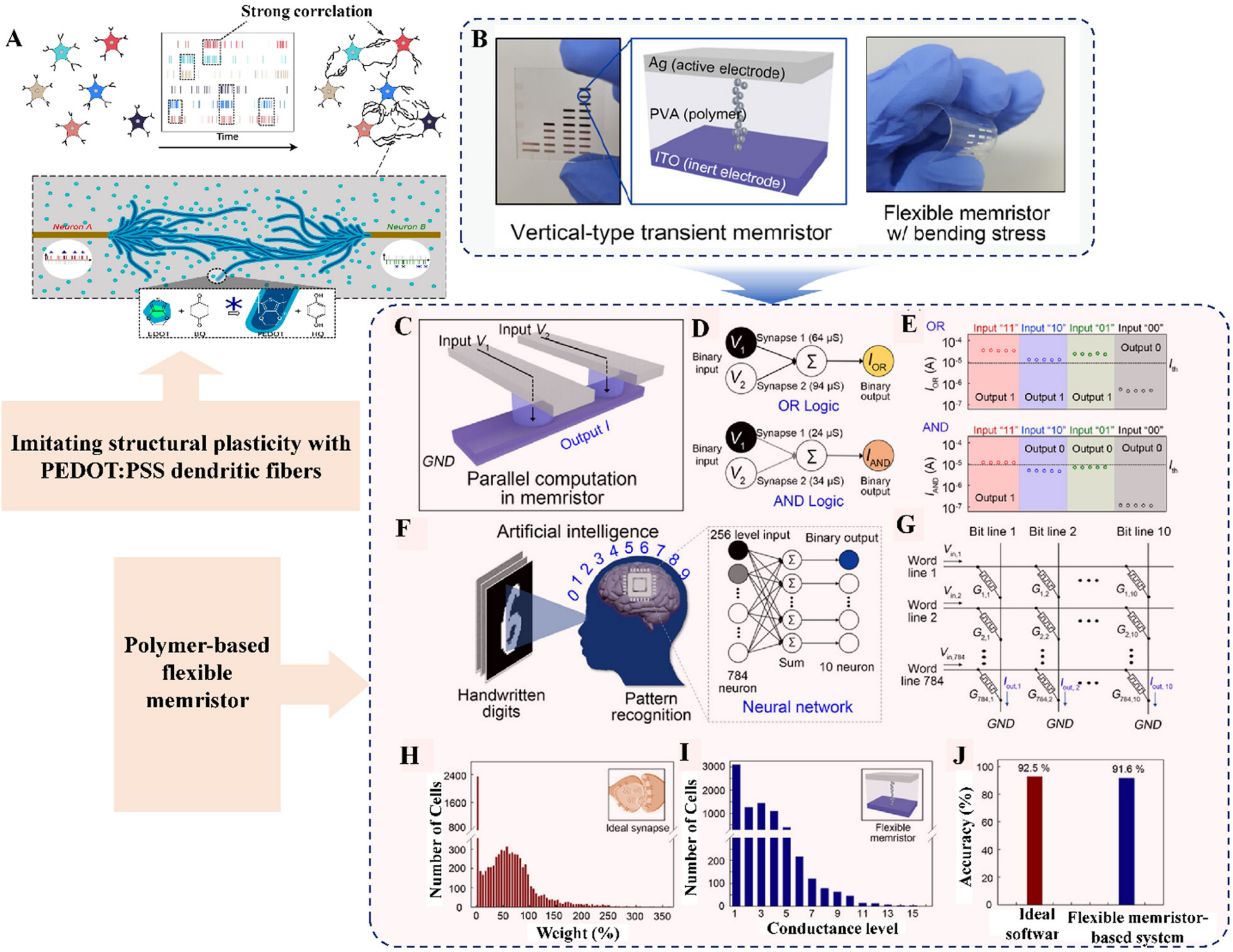

Fig. 5 (A) Dendritic electro polymerization imitating biological neural networks by applying an electrical signal. Reproduced with permission from ref. 124. Copyright 2023, (CC BY 4.0) Nature Publishing Group. (B) Vertical-type memristor on glass substrate and a poly(vinyl alcohol) (PVA)-based flexible memristor. (C) Schematic representation of parallel computation in a memristor array. (D) Neural network for logic operations OR and AND. (E) Synapse cell made by AND and OR. (F) An illustration showcasing the hardware-driven neural network for interpreting digits. (G) Crossbar array of a flexible memristor. (H) Synaptic weight distribution to read the numbers written by hand. (I) The constructed memristor array's conductance dispersion. (J) Recognition of pattern effectiveness after 50 epochs of learning in a perfect software framework and the hardware-driven neural network with the adjustable memristor. Reproduced with permission from ref. 125. Copyright 2023, Wiley-VCH.

elements and creating a thorough assessment system for the device performance remains an unresolved issue.

3.3. Organic–inorganic based devices

Consequently, one might think that the fusion of organic and inorganic substances in materials research may offer a broad range of possibilities for enhancing the functionality of neuromorphic devices. Recently, the use of organic–inorganic halide perovskites (OHPs) for the production of optoelectronic devices has skyrocketed. OHPs have excellent optoelectronic features including substantial charge carrier mobility, adjustable bandgaps, significant absorption coefficients, and long carrier diffusion lengths.[128–130] OHP properties may be adjusted using the chemical formula ABX_3 (where A = organic cation, B = metal cation, and X = halide anion).[131]

Multiple studies have shown that OHPs can be used as artificial nociceptors with remarkable homogeneity, adaptability, memory of previous injuries, and pain sensitivity.[132,133] This signifies a major advancement in the pursuit of complete neuromorphic computations and precise information processing in the human brain. Fig. 6A shows the basic layout of a nociceptor system that uses $MAPbI_3$-(methylammonium lead iodide) OHP, with OHP layered on top of a uniformly flat ITO substrate.[132] Trung *et al.* used ZnO nanorods, PEDOT:PSS, and polyurethane fiber to create fibrous photonic artificial synapses (FAPS).[134] The fabrication process of the FAPS included the deposition and patterning of an organic p-type semiconductor film made of PEDOT:PSS coated onto a Au (gold) electrode (Fig. 6B). Subsequently, ZnO nanorods were grown on a PEDOT:PSS tube using a hydrothermal method (Fig. 6C). Fig. 6D illustrates the flexibility and fiber-shaped nature of the FAPS, which can be wrapped in tubes and sewn onto the fabric without experiencing significant malfunctions. One may attempt this manufacturing procedure in their laboratory and assess the results independently because it is relatively easy. The authors suggest that this architecture could greatly minimize power usage, resembling biological photoreceptors. The device can also be integrated into fiber-based artificial synaptic arrays, making it suitable for image recognition and memory.

Nevertheless, certain factors must be considered while using OHPs.

(1) Although organic materials provide greater flexibility, their performance may be severely affected by environmental variables (such as humidity and thermal instability) when hybrid materials are used for device fabrication.[135]

(2) The intrinsic instability and poor mobility of organic materials can affect the reliability of devices and their ability for integrating synaptic device arrays and accurately imitating real synapses.[136,137]

(3) The resistive switching mechanism, which potentially affects the operational efficiency of memristors, has not been extensively studied.[138]

(4) The toxicity of lead-based devices is a serious environmental concern.[131]

3.4. Perovskite QD-based neuromorphic devices

Nanomaterials with different shapes, such as nanowires and quantum dots (QDs), can effectively convert light into electricity and operate across a broad spectrum, resulting in optoelectronic synaptic devices.[139–141] PQDs have recently attracted considerable attention as cutting-edge optoelectronic materials.[142,143] This is because they have excellent optical and electronic properties, such as low exciton binding energy, long lifetime, comprehensive spectral coverage, and high efficiency, which show that they could be useful as optoelectronic devices.[144–147] Some extensive research has been conducted on neuromorphic computing in recent years, focusing on the characteristics of perovskites.

Wang *et al.* utilized $CsPbBr_3$ QDs as the main component with other material combinations (Si/SiO_2/PMMA/pentacene/Au) to develop flash memory (Fig. 7A), where the pentacene and $CsPbBr_3$ materials had a type-II band alignment, which separated the excitons at the interfaces.[148] Flash memory devices made of $CsPbBr_3$ QDs (functioning as floating gates) trap charged particles optically and release them electrically based on the type-II band alignment between pentacene and $CsPbBr_3$, which causes excitons to separate at the interfaces. Synaptic devices using a floating-gate construction often provide benefits such as prolonged memory retention and a gate-tunable effect. Nevertheless, the deposition operations of multilayer

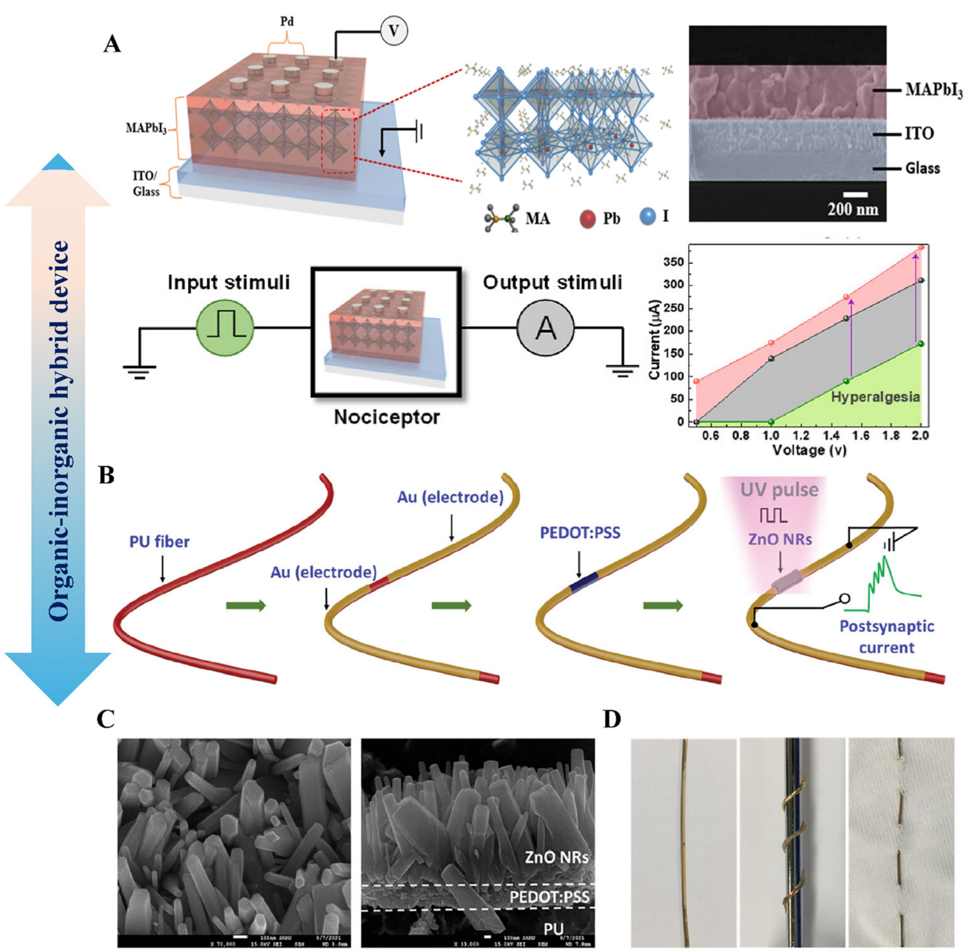

Fig. 6 (A) Schematic representation of a Pd/$MAPbI_3$/ITO memristive gadget for artificial nociceptors with a cross-sectional SEM image. Reproduced with permission from ref. 132. Copyright 2023, American Chemical Society. (B) FAPS fabrication process. (C) FE-SEM micrograph of ZnO NRs/PEDOT:PSS/PU (top and cross-sectional view). (D) FPAS as fabricated, twisted on tubes, and stitched on textile photographic images. Reproduced with permission from ref. 134. Copyright 2023, Wiley-VCH.

materials might amplify the intricacy of fabrication. Additionally, the thickness of the top sedimentary material affects the light absorption by the perovskite material.[149] Furthermore, when used as a conduction layer, the total charge conductivity of perovskites tends to be relatively low, particularly in cases where the gate effect cannot be produced. These characteristics require a high operating voltage to provide a sufficiently high response current, thereby increasing the electrical energy utilization.

Hao *et al.* introduced a photonic synaptic transistor (Fig. 7B) fabricated using an organic semiconductor with $CsPbBr_3$ for an artificial visual system application.[150] As per the author's findings, combining $CsPbBr_3$ QDs with organic semiconductors can improve synaptic behavior. This is because of the significant energy barrier between the valence band (VB) of $CsPbBr_3$ QDs and the highest occupied molecular orbital (HOMO) of the organic semiconductor material. In addition, the presence of charge traps within the channel or at the interface leads to a low rate of combination of photogenerated charge carriers, resulting in excellent synaptic performance.

However, there are additional challenges, such as the precise engineering of the interface between the floating gate and charge-transporting material and ensuring suitable energy offsets. In addition, selecting a photoactive material with a long exciton lifespan is crucial for enhancing the efficiency of the charge separation process. Chen *et al.* described the photophysical properties of a floating-gate function in photo memory. They used P3HT (poly(3-hexylthiophene-2,5-diyl)) a p-type semiconducting polymer, along with a silicon substrate, and a simple A-site substitution method (Fig. 7C) for rapid responsiveness and minimal energy consumption.[151] Similarly, Ercan *et al.* investigated photonic synaptic transistors with a low energy consumption.[152] They fabricated these transistors using QDs and P3HT, with composite nanofibers (CNFs) serving as semiconducting channels (Fig. 7D). This approach provides a convenient means for developing high-performance electronics, including memory and visual perception systems that mimic human capabilities, as well as advanced optical communication systems. In addition, Gupta *et al.* used a material combination (QDs/P3HT) comparable to that reported in a previous study using doped Si and a SiO_2 layer (Fig. 7E).[153] They successfully created trap-assisted optical synapses that enhanced the detection efficacy of a neuromorphic system.

Most metal halide perovskites (MHP) used in memory registers switch symmetrically, which can cause significant leakage current problems when building an array.[155] During these situations, the change in states could cause the updating process to stop working because it sets off unwanted pathways at the level of the neural network array, resulting in less effective learning efficiency.

In a recent study, Park *et al.* used mixed-dimensional perovskite QD heterostructures in artificial neural networks to create neuromorphic electrical functions that make networks better at learning and use less energy.[154] The fabrication of a mixed-dimensional stack junction between and ITO electrodes is shown in Fig. 7F. The Al and ITO electrodes in this arrangement represent the axons of a pre-neuron (grey) and the dendrite of a post-neuron (yellow), respectively. When a presynaptic pulse (VINPUT) was applied to Al, a postsynaptic current (PSC) was created in the ITO using a mixed-

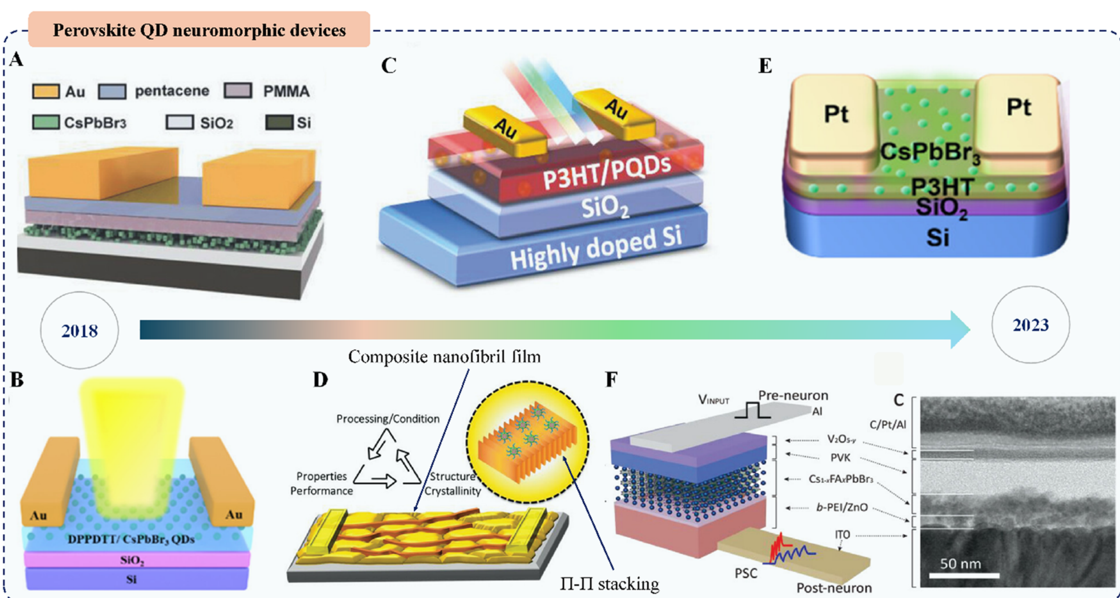

Fig. 7 A 3D schematic of (A) flash drive based on $CsPbBr_3$ QD. Reproduced with permission from ref. 148. Copyright 2018, Wiley-VCH. (B) DPPDTT/$CsPbBr_3$ QDs synaptic transistor. Reproduced with permission from ref. 150. Copyright 2020, American Chemical Society. (C) P3HT/PQD-based photomemory device. Reproduced with permission from ref. 151. Copyright 2021, Wiley-VCH. (D) photonic FET memory devices comprising CNFs. Reproduced with permission from ref. 152. Copyright 2021, Wiley-VCH. (E) SiO_2/$CsPbBr_3$/P3HT based transistor structure. Reproduced with permission from ref. 153. Copyright 2023, American Chemical Society. (F) Cs_{1-x} FAxPbBr$_3$ QD-based synaptic gadget with a cross-sectional HR-TEM micrograph. Reproduced with permission from ref. 154. Copyright 2023, Wiley-VCH.

dimensional stack design. They also reported that the energy band of a synaptic device based on mixed-dimensional perovskite QDs was influenced by the size of the QDs. The interaction between the energy bands is affected by modifying the size of the QDs, which in turn affects the transport of charges and the manipulation of primary synaptic functions. Therefore, the dimensions of the QDs can be regarded as a key technical parameter for synaptic devices using mixed-dimensional QDs. This study revealed a favorable approach for the development of high-performance synaptic devices utilizing mixed-dimensional halide perovskite QDs.

4. Applications

4.1. Comparison of single and multi-sensory systems

An advanced sensing system consists of multiple sensor components and a pattern-recognizing unit that collects data and uses neural-network-based software to detect, evaluate, and make judgments. A neural network or comparable pattern recognition tool is crucial because the sensor arrangement is nonlinear and requires calibration.[156,157] Machine learning (ML) algorithms have been widely used to study the sensory system in neuroscience, particularly in healthcare applications, due to their promising applications such as blood pressure estimation,[158] recognition of silently spoken words,[159] detection of human motions,[160–163] and object recognition.[164–168] There are two types of sensor devices that are determined by the number of output signals: single- and multisensory devices.

A single-sensory system uses only a single output signal from a sensor to extract features, whereas a multisensory system uses several output signals of one or multiple sensing types. Using machine learning techniques, a single sensory system can detect a specific input, including pressure, strain, tactile feedback, and other mechanical or health-related information.[169–171] This type of system enhances user comfort by enhancing usability and mobility using machine-learning-assisted data interpretation with a single signal.[172,173] However, some limitations must be discussed, such as neuromorphic devices with a single sensory system, which may struggle to multitask and integrate information across modalities, thus restricting their application.[159,160] For example, a neuromorphic tactile system can adapt to process and analyze touch signals but may not be able to integrate the visual characteristics or shape of the object. Most of the current research on neuromorphic systems or devices focuses on a single pattern-recognition challenge, limiting future advancements to a broad spectrum of applications.

With the rapid development of biomimetic devices, incorporating AI into sensory systems requires a multidimensional sensing device. Multimodal sensors collect data from several modes to analyze signals. These multimodal descriptions provide a more thorough representation of the multiple dimensions of an identical object activity, thereby enhancing the model's knowledge and cognitive capacity. This implies that a multisensory strategy is more beneficial for maintaining high prediction accuracy than a single sensory system. Table 1 presents a comparison of the algorithms used in single- and multi-sensory systems, along with their respective advantages. Some recently developed multisensory devices include sensory memory processing systems (SMPSs) to detect multi-wavelength light emission and multimodal data processing,[174] all-polymer electrochemical transistors (AECTs) to identify touch and taste,[175] OHPs synaptic transistor for emulating photoelectric synaptic activity and showcasing an artificial reflex arc,[176] artificial multisensory integration nervous (AMIN) systems to detect tactile and iconic perception behavior,[177] and oxide-based memcapacitor (OMC) to operate data related to visual, aural, electrophysiological, and mechanical features.[178] Although multiple signal integration has been shown to improve prediction accuracy in ML models, the following challenges need to be recognized while developing a multi-sensory system:

(1) Challenges in data processing performance emerge as the volume of data grows.[179]

(2) Sophisticated neural algorithms must be incorporated into neuromorphic devices.[30]

(3) Real-time imitation of biological neuronal systems is performed using artificial neuromorphic prosthetic devices.[180]

(4) A neuromorphic system for multidimensional signal processing requires exceptional consistency.[181]

(5) Cross-sensitivity needs to be reduced to ensure accurate measurements.[169]

4.2. Multi-sensory neuromorphic device

As humans acquire external inputs from their surroundings, sensory receptors detect and transform these sensations into nerve impulses conveyed to matching brain regions, thereby enabling humans to interact with their surroundings.[182] Multi-sensory integration refers to the combination of information from several sensory streams to create holistic awareness. This integration helps clarify the differentiation of external stimuli and enhances responsiveness.[183] In contrast, using a single sensory input in an artificial computer system for decision-making often results in inherent uncertainty due to the random nature, biased characteristics, and signal processing noise.[184] For example, a multisensory device can detect varying degrees of congruence between a participant's vision, touch, and proprioception; for instance, when a knife dexterously glides across a fake hand and the participant simultaneously experiences pain and danger. This congruence enables participants to perform more complex recognition or decision tasks.[185,186] Multi-sensory integration offers another advantage known as the "inverse effectiveness effect."[187,188] Highly noticeable stimuli in one sense activate the corresponding neurons, making them easily detectable. However, it is difficult to detect weak signals using a single sensory system.[189] In such cases, multisensory integration can significantly boost neural activity and the chances of detecting and locating events. Some of the recently developed multi-sensory integrated systems are discussed below.

An artificial sensory neuron utilizes a combination of sensing processes to detect and analyze distinct patterns of a fingerprint. It then determines whether the fingerprint is

Table 1 Comprehensive summary of single and multisensory systems with ML algorithms and their applications

Types	Algorithm	Sensing type	Application	Advantage	Ref.
Single sensory system	FNN	Pulse signal	Real-time blood pressure estimation	The results were highly reliable with a small mean deviation of $<3\%$ with commercially available devices	158
Single sensory system	LDA, Linear SVM, Quadratic SVM, Gaussian SVM, *K*-nearest Neighbors	Triboelectric signal	Recognition of the real-time silent spoken word	The Gaussian SVM model yielded the highest word classification accuracy of 99.2%	159
Single sensory system	LSTM	Pressure	Biomechanical action level classification in a smart mask	The smart hybrid sensor for biomechanical motion detection with an overall accuracy of $\sim$88%	160
Single sensory system	LSTM	Strain	Identifying complex hand motion	To maximize user convenience in terms of usability and mobility, a sensor with a single channel was used to produce signals	161
Multi-sensory system	AlexNet CNN and sparse neural network	Somatosensory (strain) and visual sensory (camera)	Hand gesture recognition	Bioinspired somatosensory–visual associated learning achieved the best recognition accuracy (100%) compared with visual-based recognition (89.3%) and somatosensory-based recognition (84.5%)	162
Multi-sensory system	CNN	Breathing pressure	Recognition of respiration types	The collection of respiratory signals from multiple channels demonstrates superior recognition of respiration patterns when compared to that of a single channel	163
Multi-sensory system	CNN	Pressure and temperature	Object recognition using tactile glove	The multi-sensory system, incorporating both pressure and temperature signals, achieves an accuracy rate of 94.9%, surpassing the 85.65% accuracy rate of a single sensory system focused only on pressure	164
Multi-sensory system	CNN	Tactile and olfactory	Human identification in rescue conditions	In contrast to visual perception, a multi-sensory sensing system involving tactile and olfactory presents an alternative method in dark or blocked environments, demonstrating its superiority in identifying humans during rescue operations	165
Multi-sensory system	MLP	Thermal conductivity, contact pressure, object temperature, and environment temperature	Object recognition in object size, shape, and material	Integrating pressure sensing alongside thermal conductivity and temperature sensing as a multimodal system significantly enhances the accuracy of object classification, resulting in an overall accuracy of approximately 96%. In contrast, relying solely on thermal conductivity sensing yields a total accuracy of about 68.1%	166
Multi-sensory system	CNN	Bending, contact position, and temperature	Digital-twin-based virtual shop	In contrast to isolated values, the 15-channel spectrum in the time domain for one gripping motion may contain more hidden information. These data serve as a valuable feature of each sample, contributing to enhanced classification accuracy	167
Multi-sensory system	LDA	Triboelectric signal	Material recognition	With data initially sourced from a single channel, sample clustering appeared less structured, resulting in a classification accuracy of 52.7%. However, as the number of channels increased, the clustering of samples became more distinct with a classification accuracy of 96.8%	168

LSTM (long short-term memory), FNN (feedforward neural network), SVM (support vector machine), CNN (convolutional neural network), MLP (multilayer perceptron), LDA (linear discriminant analysis)

genuine, originating from real skin, or counterfeit, originating from synthetic skin. Han *et al.* used light to discern the distinctiveness of a pattern, whereas body heat was used to confirm its validity (Fig. 8A).[190] In another study, Liu *et al.* proposed a multisensory system that utilized electrolyte-gated vertical organic field-effect transistors (VOFETs) to make artificial tongues.[191] It can perform numerous functions such as recognizing, responding, and imitating the behavior of biological sensory systems. The author explained this concept with some easy steps, in which biological receptors perceive environmental stimuli and transform them into electrical impulses (Fig. 8B). Signals were sent *via* a sensory transduction network and transmitted to the cerebral cortex for additional evaluation and comprehension. The preneuron transmits presynaptic spikes to the synapses in response to an external input. Subsequently, neurotransmitters in the presynaptic layer propagate toward the postsynaptic membrane, creating a postsynaptic current. Their findings could be improved by detecting the mechanism for multiple objects (*e.g.*, acetic acid, alcohol, and ether) instead of just one. In addition, there needs to be a mention of why the artificial tongues feel pain (as discussed in the literature) when increasing the acetic acid concentration, as the author only showcases the results without explaining whether this device only works for acidic materials and will be similarly helpful for other materials (*i.e.*, alcohol and ether) or if the device is pH-responsive.

Fig. 8C shows a schematic of a multisensory system (visuo-tactile) for visual and touch information in the human neurological system.[192] The tactile sensor used in the demonstration consisted of an array of readily available Kapton and aluminum foils with an air gap between them. Upon contact between two different materials, the triboelectric phenomenon generates electrical impulses *via* charge transfer, thereby achieving a tactile response. The sensation of touch is made possible through the triboelectric phenomenon. This involves the generation of electrical impulses when two materials with different properties come into contact. The amount of electrical impulse produced by the triboelectric tactile sensor directly correlates with the surface charge, which is influenced by the area of contact. The author also discussed the concept of the inverse effectiveness effect, explaining that highly noticeable sensory stimuli can elicit strong reactions in corresponding neurons. This effect is caused by the triboelectric gate voltage, generated from touch stimuli, being affected by the confined charges at the interface created by visual stimuli. As the visual stimuli become stronger, more photo-generated carriers are trapped at the contact, resulting in a higher detection of the triboelectric voltage. Although the author claims that this principle can be applied beyond visuo-tactile information, the literature has primarily focused on tactile sensing using conventional tactile sensor concepts, with no proper explanation for the detection and interpretation of visual sensing signals.

In general, the integration of multisensory reception is severely restricted owing to the challenge of effectively linking sensors and synapses.[195] Despite this challenge, researchers continue to explore several multisensory systems, including multifunctional neuromorphic e-skin *via* organic transistors,[196] visual-haptic cognitive systems using photodetectors,[197] and bioinspired multisensory neuronal networks[198].

In a recent study, He *et al.* introduced ML materials and optoelectronic synapses (InGaZnO/methylammonium lead iodide) for detecting visual and tactile information (Fig. 8D).[193] ML materials facilitate tactile awareness by converting tactile sensations into discernible light, which alters the optoelectronic synapse weights. According to the author, light pulses help evaluate the device's neuromorphic light-interactive behavior, directly linking it to neuronal communication. When combined and transformed into postsynaptic currents, these pulse signals mimic how neurons transmit information. Modifying this current's pulse width, pulse quantity, and pulse rate is essential for

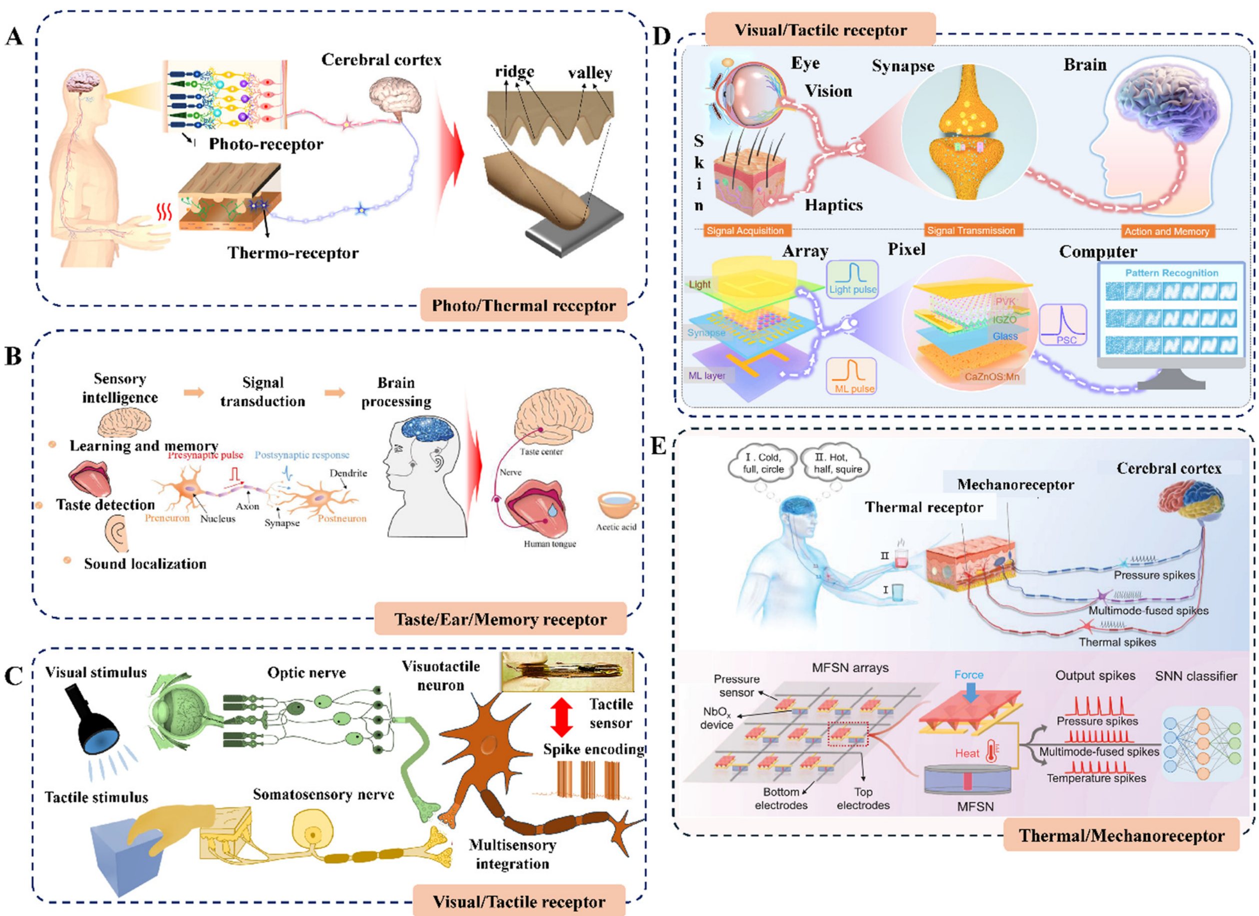

Fig. 8 (A) Biological photo-thermal receptor for fingerprint recognition. Reproduced with permission from ref. 190. Copyright 2023, American Chemical Society. (B) Representing perceiving and interpreting external inputs for taste and sound detection. Reproduced with permission from ref. 191. Copyright 2022, Wiley-VCH. (C) The biological neuronal system's multimodal processing of visual and touch inputs. Reproduced with permission from ref. 192. Copyright 2023, (CC BY 4.0) Nature Publishing Group. (D) Visual/Tactile system for a human (top) and artificial (bottom) synapse network. Reproduced with permission from ref. 193. Copyright 2023, Wiley-VCH. (E) Schematic diagram of a biological somatosensory system (top) and artificial somatosensory system (bottom). Reproduced with permission from ref. 194. Copyright 2022, Wiley-VCH.

replicating the brain's functions, particularly those related to memory formation and decision-making processes. The author asserts that the device effectively identifies written digital files by emulating an artificial neural network combined with a ML algorithm. It achieved an identification precision of 70% for visual–tactile fusion, suggesting its potential for applications in flexible frameworks and mechanically compliant structures. Despite notable improvements, one can argue that distinct sensory and processing unit setups give rise to problems related to network convergence, spatial accuracy, and data transfer delays. Therefore, researchers have mainly focused on combining the detection, analysis, learning, and memorization functionalities into a single device to enhance artificial perceptual systems.

According to Won *et al.*, the traditional artificial sensory system analyzes various types of information using a centralized and successive computing structure. This process requires the conversion of multimodal sensing signals into digital format before the digital processor can be analyzed.[199] As a result, this approach requires significant hardware space, power usage, and communication bandwidth. Recently, Zhu *et al.* designed an artificial multimodal sensory device using a spiking neural network (SNN) classifier and a group of multimode-fused spiking neurons (MFSNs) that work in the spike domain. Their methodology included detecting anomalous temperatures and intense mechanical stimulation by analyzing spike trains that transmit mechanical stimuli and temperature data. These signals travel to the cerebral cortex, where multimodal information is processed and combined to make precise judgments (Fig. 8E).[194]

Some recent reports also suggest that researchers are constantly trying other approaches, such as Brainoware with the help of brain organoids[200–202] (self-organizing pluripotent stem cells from humans can form brain-like tissue that can imitate the structure and functioning of a growing brain), to perform voice recognition by differentiating the vowels of a certain speaker.[203] However, several issues may arise with this strategy, and an inherent technological obstacle lies in the production and maintenance of organoids. Furthermore, this effectively preserves and facilitates the development of organoids that harness computing capabilities. These findings suggest that using a multimodal technique is more advantageous than using a single sensory system for sustaining high prediction accuracy.

4.3. Spike-based VO_2 memristors

The architectural characteristics of most brain structures that provide benefits include extensive interconnections between neurons, coexistence of neural processing and consciousness, and the use of spikes for communication.[204,205] The primary emphasis of the algorithm development for spike-based neuromorphic gadgets has been their applicability to deep neural networks and other developing AI algorithms.[11,206–208] As AI algorithms draw inspiration from the brain, the utility of neuromorphic computing is expected to increase.[11,209] According to synaptic connection topologies, some spike-based neuromorphic systems include neurogrids,[210] TrueNorth,[204] SpiNNaker,[205] BraneScales,[211] and Dynap-se,[212] computer architectures that emulate communication between organic neurons using spikes.

To develop a successful neuromorphic device, it is essential to understand how biological neurons behave when neuro signals are transmitted to an artificial network. The following are some examples of recently developed memristors: first, neuromorphic devices made of silicon nanosheets,[213,214] and second, devices made using a pulsed laser-fabrication process.[215–217] However, silicon-based devices face challenges such as high energy consumption and low device efficiency.[217–219] Later, laser-fabricated devices became an alternative option for achieving better energy consumption and efficiency. Some recently fabricated devices include the following: a VO_2 (vanadium dioxide) locally active memristor has the benefit of emulating neural behaviors more realistically in biological neuromorphic systems.[220] This is because they can closely mimic the behavior of neurons. Nevertheless, they fail to provide a theoretical explanation of the memristor properties or illustrate the oscillation behavior. Hence, it is crucial to better understand the functioning of neurons using network models and quantitative analytical techniques to investigate the dynamics of neuromorphic systems.

Yuan *et al.* recently demonstrated the simple integration of an asynchronous spike encoder and long short-term memory spiking neural network (LSNN)-based decision system in VO_2 memristor-based neuromorphic processing (Fig. 9A).[221] The memristor-based asynchronous spike encoder converts physiological signals such as electrocardiogram (ECG) and electroencephalogram (EEG) into two-channel trains while compressing and encoding the data. According to the authors, their temporally encoded system was more neuromorphic-friendly than frequency-encoded neurons. The frequency of spike production depends on the rate of change of the original input signal. The greater the rate of change of the initial input signal, the stronger the spikes. This encoding method is advantageous because it produces sparse spikes which lowers the quantity of data required and minimizes the consumption of energy. Because asynchronous spike trains maintain the signal information, they can adequately recover the original signal, which is difficult for frequency coding. Wang *et al.* identified comparable characteristics, wherein the implementation of a temporally encoded system substantially enhanced the information and energy efficiency of neuromorphic hardware.[222]

In some cases, pulsed laser deposition is used to develop an epitaxial VO_2 memristor that functions as a calibratable artificial sensory neuron (CASN).[181] This neuron converts sensory signals from various receptors (such as photoreceptors, thermal receptors, and mechanoreceptors) into electrical spikes. Neurons transmit these electrical spikes to process them in a SNN (Fig. 9B). The cerebral cortex processes neural impulses in response to external stimuli. The VO_2 memristor exhibits volatile resistive switching behavior, transitioning between high and low resistance when the applied voltage surpasses a certain threshold. Epitaxial VO_2 memristors feature threshold-switching capabilities used in spike neuron implementation. Fig. 9C shows the dynamic network structure of the brain, which processes and stores signals using readily controllable

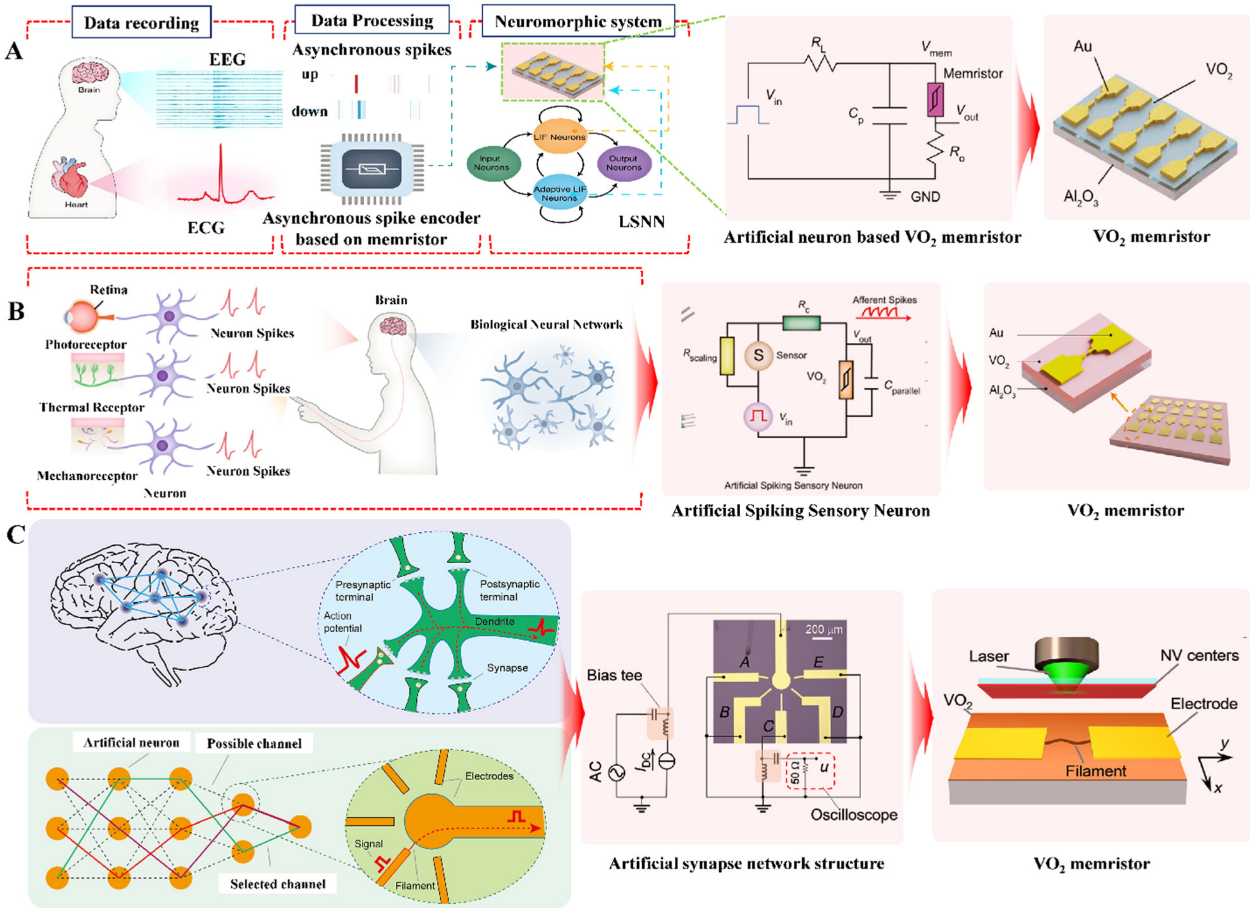

Fig. 9 (A) Artificial neural signaling system constructed using a VO_2 memristor for human machine interfaces. Reproduced with permission from ref. 221. Copyright 2023, (CC BY 4.0) Nature Publishing Group. (B) VO_2 spike-based neuromorphic multi-sensory system. Reproduced with permission from ref. 181. Copyright 2022, (CC BY 4.0) Nature Publishing Group. (C) Human brain inspired dynamic network structure for signal transmission using a VO_2 memristor device. Reproduced with permission from ref. 223. Copyright 2023, (CC BY 4.0) AAAS.

programmed paths that follow nervous system algorithms made by VO_2 films grown on aluminum oxide (Al_2O_3).[223] The artificial synaptic network consists of a circular electrode, which serves as a common terminal. This electrode imitates a biological dendrite and is connected to a DC, bias tee, and channels A, B, C, D, and E. Their argument indicated that the network can be arranged hierarchically, creating a dynamic neuromorphic framework facilitated by laser-controlled filament positioning with nonvolatile memory. The connectivity pathways in these neuromorphic structures can be readily manipulated, resulting in inherent memory capabilities based on imprinted conduction routes similar to those observed in organic nervous systems. Despite the VO_2 memristor having certain benefits, the currently developed systems do not exhibit a high level of efficiency for neuromorphic systems, as they are still in the experimental stage.

However, it can enhance the progress of hardware neural network structures with brain-inspired algorithms while enabling the implementation of neuromorphic computing. Furthermore, the research now constrains several aspects of efficient sensing of neuro signal and signal fluctuation concerns, substantiating their applicability in practical neuromorphic device implementations. Moreover, the firing rate of individual neurons contributes to the potential degrees of freedom in network structure dynamics.[224] A multidimensional space represents the activity of individual neurons and the path from an input to an output represents the response of the neuron. Consequently, despite its importance, contemporary research faces substantial obstacles regarding the process of signal filtration for individual neurons. Regardless of these challenges, the development of effective human-machine interfaces utilizing neuromorphic systems is of considerable interest to researchers.

4.4. Application in an artificial vision system

The sense of sight detects 80% of the information among all external stimuli.[225] As a result, when it comes to observation, the retina is among the most important parts of the human body. Emulation of a human retinal system has served as a source of inspiration for both device fabrication and research, along with signal-processing algorithms.[226,227] These advancements have the potential to enhance AI and the Internet of Things (IoT) in the future.

4.4.1. UV light recognition and visualization. Ultraviolet (UV) radiation, with a wavelength of 10–400 nm, may have detrimental effects on the skin, leading to premature aging and skin malignancies.[228] The intensity, duration, and amount of exposure to ultraviolet (UV) radiation determine the severity of these disorders.[229,230] Therefore, the development of photonic synapses that mimic the functionality of the retina and enable selective detection and processing of ultraviolet (UV) inputs is crucial for expanding human visual perception beyond the range of visible light.

Park *et al.* used carbon nitride treated with nitric acid (NT-CN) to establish a photonic synaptic transistor sensitive to UV light (Fig. 10A).[83] The device fabrication method involved the formation of a thermally generated SiO_2 film on a Si wafer. They used NT-CN on an SiO_2 surface as a UV-responsive interface layer. They applied poly(methyl methacrylate) (PMMA) to the NT-CN film for planarization of the NT-CN layer and as a tunneling substrate. Pentacene served as the organic semiconductor, whereas Au functioned as the electrode material.

The proposed principle for the device is that when exposed to UV light, both the NT-CN and pentacene films produce photoinduced electron–hole pairs (EHPs) (Fig. 10B). The holes generated by photoexcitation tunnel through the PMMA layer and enter the pentacene film. Conversely, the photoexcitation process confines electrons inside the NT-CN films, creating a negative potential that increases the drain current. Upon removal of the UV light, the photoinduced EHPs in the pentacene film undergo rapid recombination. In contrast, the trapped electrons in the NT-CN film cannot promptly recombine with the holes, resulting in a prolonged recombination period. This delay was responsible for the observed synaptic properties. However, the author overlooked a crucial aspect of their analysis, particularly the presence of substantial noise in the raw UV data reflected by the target item.[232,233] Li *et al.* identified pentacene as a charge-transport material because of its molecular structure, which is an important parameter in memory devices.[234]

Moreover, owing to the elevated noise level of the initial UV image information, residual background noise often persists even after the traditional in-sensor preprocessing stage. Hence, there is a need for a new UV imaging system that can perform precise vision identification with minimal image filtering during the backend analysis phase.[235,236] Seung *et al.* demonstrated the use of a synaptic phototransistor-quantum-dot light-emitting diode (SPTr-QLED) to extract preprocessed images from frequent and strong optical signals (Fig. 10C).[231] The author further elucidates recognizing images using a deep neural network. They emphasize that background noise in target photos can lead to inaccurate detection because the neural network is trained on a standard dataset of raw images with little noise. Specifically, considering the significant amount of noise in unprocessed UV photos, it is essential to minimize background noise for precise image identification. The preprocessing effectively reduced background noise and improved the image recognition accuracy. The SPTr-QLED can produce a preprocessed picture with less background noise without needing extra image-filtering steps in the back-end processing. This was achieved through on-device preprocessing using a signal or none (SoN) approach. SPTr produces a weighted photocurrent owing to consecutive noisy ultraviolet (UV) inputs. Current-to-voltage converters connect the SPTrs and QLEDs electrically such that the weighted photocurrent can be changed to the postsynaptic voltage. The QLED module uses this voltage as input. The QLEDs exhibited an exponential rise in current when subjected to an input voltage, resulting in enhanced contrast in both the electrical and visual outputs (Fig. 10D). Nevertheless, the authors' findings indicated that the recognition rate achieved in the simulation was 86.2%, whereas for in-sensor preprocessed images, it was only 49.7%. This suggests that traditional synaptic photodetectors (SPD) are inadequate for accurately recognizing noisy UV images. Therefore, additional noise filtering is required to achieve a high recognition accuracy. However, their findings have guided researchers in decreasing the hardware complexities of SPD and enhancing their efficiency.

4.4.2. Neuromorphic devices for color recognition. Traditional photodetectors convert incoming light stimuli into electrical impulses in real time; however, their quick recovery makes it difficult to store, recall, or preprocess any input information.[237,238] In contrast, the human visual system relies on the optic nerve, which transmits visual data from the retina to the brain for processing and storage.[239] The immediate reaction to stimuli in the brain allows synaptic strengthening *via* neuronal signaling, which in turn allows for the memory of that information.[240,241]

The use of optical color filters to categorize incoming wavelengths limits the effectiveness of artificial retinal systems, resulting in a low pixel density and significant spectrum absorption loss.[242,243] Nevertheless, most studies on photosynaptic devices rely on monochromatic optical stimulation.[244] Weak or strong photoconductivity of active semiconducting materials makes many color recognition synaptic systems possible. However, when exposed to light, many of these systems struggle to select specific light wavelengths.[245,246] Therefore, achieving more effective color vision through multispectral selectivity by regulating neural plasticity is an interesting prospect.

Jo *et al.* introduced an artificial photonic synapse that utilizes a precise QD mixing ratio to achieve quantitative tuning.[247] This synapse enables wavelength-specific responses in a single pixel, enabling enhanced color selectivity to distinguish between optical wavelengths of varying intensities. The process of imitating color recognition included creating a 7×7 grid of pixel arrays using a combination of mixed QDs (M-QDs) and amorphous indium–gallium–zinc–oxide (a-IGZO) phototransistors (Fig. 11A). The constructed array structure provided specific voltages to each data and gate node while keeping the source node neutral. Their investigation focused only on identifying red, green, and blue (RGB)-color images using three distinct modes: RGB, GB, and B (Fig. 11B). According to the author, a critical factor in color perception is the transition from nonvolatile to volatile properties over the visible light spectrum. The identification rate increased as the pulse number increased until the 30th pulse was reached. However, after

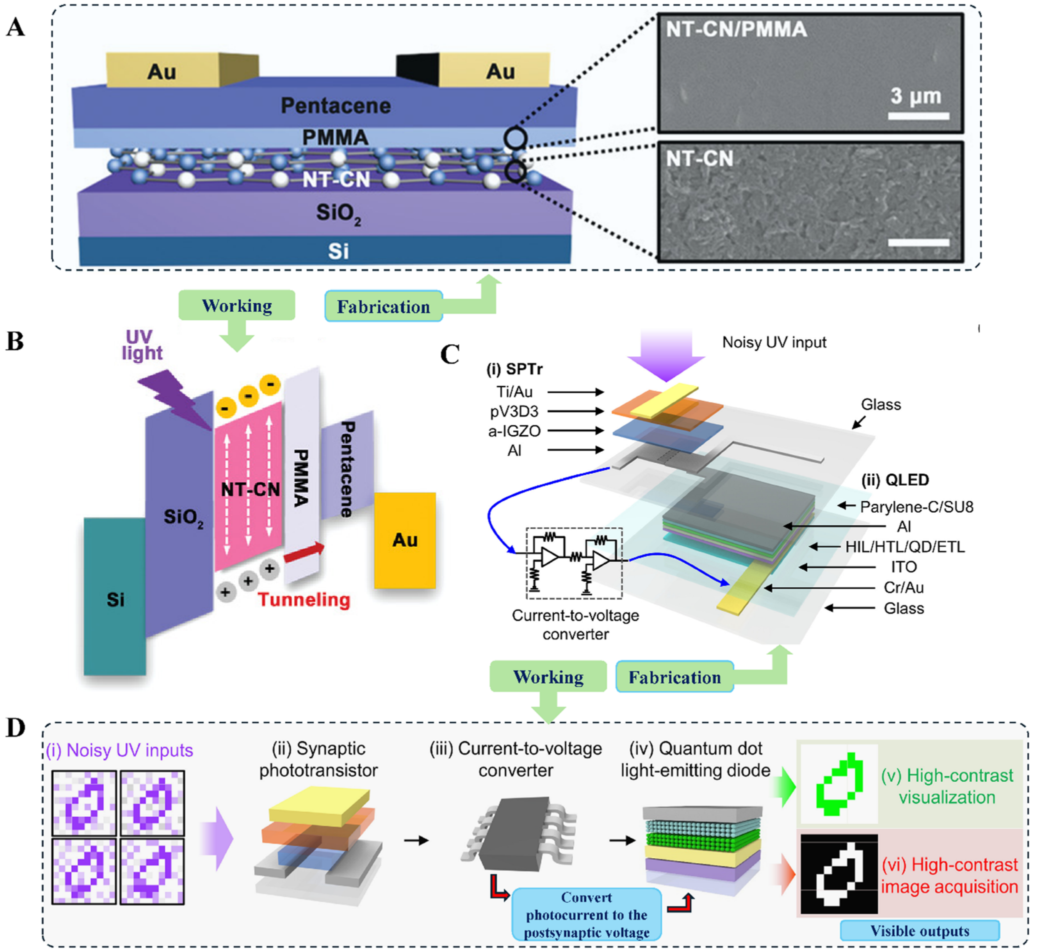

Fig. 10 (A) The structure of CNUVS is shown in the left panel, along with each of its components with SEM micrographs of NT-CN and NT-CN/PMMA layers. (B) Working principle of CNUVS under UV radiation. Reproduced with permission from ref. 83. Copyright 2020, Wiley-VCH. (C) Illustration depicting the internal components of the SPTr-QLED. (D) Schematic representation demonstrates integrating the SPTr-QLED to generate high-contrast visible from the chaotic UV patterns. Reproduced with permission from ref. 231. Copyright 2022, AAAS.

that point, the images started to blur, resembling the process of human memory deterioration over time. Additionally, they determined that the order of magnitude of RGB light-stimulated photosynaptic currents significantly impacted visual memory. However, further clarification is required regarding their conversion from nonvolatile to volatile for use as sophisticated artificial vision systems capable of efficient color identification and optimal pixel density. However, this study may guide researchers who want to construct replicable biological visual systems with distinct visual elements.

Along with a similar type of problem identification and the additional feature of structural recognition, Hou *et al.* introduced a RGB narrowband photodetector array with panchromatic imaging capability by primarily fabricating halide perovskite films using a volatile solution (VS) method and then utilizing a multilayer algorithm to model the human retinal system (Fig. 11C).[248] Perovskite has the benefit of the ability to manipulate its properties, namely its vast range of bandgaps.[249,250] This allows panchromatic imaging in which multiple colors may be used to display selected spectral responses within the red, green, and blue channels (Fig. 11D). The photocurrent distribution at zero bias clearly reveals the RGB characteristics of the original picture with distinct contrast and accurate representation (Fig. 11E). The authors presented two methods: (a) the channel-merging approach, which involves normalizing 2D current data to pixel intensity values with the minimum pixel value set at 0 (Fig. 11F(i)). After translating the floating-point normalized values into integers, the sunflower image was rebuilt by stacking pixel-intensity integers using RGB channels (Fig. 11F(ii)). In contrast, (b) machine learning reconstruction utilizes a multilayered perceptron neural network to forecast pixel values based on the current input data. The peak signal-to-noise ratio (PSNR) of the recreated figure from channel merging is lower owing to the sensor array setup error and measurement noise, which are intrinsically corrected and reduced by the machine learning techniques (Fig. 11F(iii) and (iv)).

Although the output may seem sustainable, some aspects might directly impact the performance of the device, including responsiveness, electron–hole transit, and material bandwidth.[251] Researchers might capitalize on the approach provided by the author to address the research deficit in this sector.

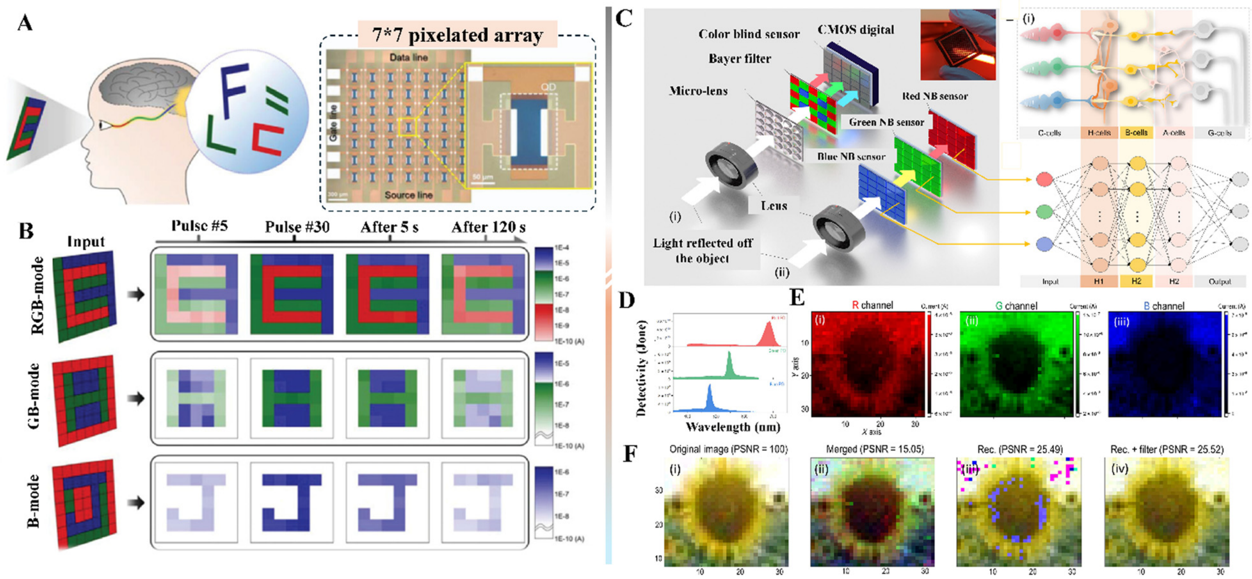

Fig. 11 (A) Pixel-based M-QD/a-IGZO phototransistor perception based on the human vision system. (B) Each array pixel's contour mapping in RGB, GB, and B. Reproduced with permission from ref. 247. Copyright 2022, Wiley-VCH. (C) Retina-inspired panchromatic imaging system. (D) Wavelength *vs.* detectivity graph. (E) Current mapping of three different channels: red, green, and blue. (F) Sunflower (i) optical image, and (ii) direct channel merging. Neuromorphic processing (iii) without filtration and (iv) with filtration. Reproduced with permission from ref. 248. Copyright 2023, AAAS.

5. Others

5.1. Butterfly-inspired multi-sensory device

Research on butterfly architectures has recently increased with respect to sensor applications.[252–258] Qualities such as refractive-index responsiveness and delicate architectural sensitivity are crucial characteristics that are the current research goals. Wing characteristics are also critical in energy-harvesting applications.[259–262] Male butterflies display vivid wing colors to entice females, who assess possible partners based on the color designs' intricacy, balance, and vividness.[263,264] Additionally, male butterflies emit chemical pheromones that are crucial for grasping female butterflies in mid-air.[265,266] These chemical signals provide essential information for species identification, mating excellence, and reproductive preparedness. Female butterflies possess specific chemosensory receptors that allow them to differentiate between various pheromone patterns.[267,268] These findings indicate the importance of a comprehensive study to enhance the understanding and create more effective bio-inspired functional materials.

Zheng *et al.* recently addressed the need for specialized hardware to gather data from various sensor elements based on the architectural design of butterflies (Fig. 12A).[269] This process involves transferring signals to the processing module, which leads to delays and increased energy consumption. Although current AI primarily focuses on visual data, it is essential to acknowledge that chemical signals can improve or change visual perception. Therefore, they built a visuochemical apparatus using molybdenum disulfide (MoS_2) and graphene-based visual and chemoreceptor neurons to analyze the data (Fig. 12B). The overall concept involves the use of various chemical solutions to achieve pheromone diversity. To demonstrate the circuit, AND and OR gates were utilized (Fig. 12C and D). Different colors (red, orange, green, and blue) of light-emitting diodes (LEDs) with varying intensities were used to imitate the hue and intensity of male butterfly wings (Fig. 12E and F). They used these colors to explain mating rejection and acceptance.

Although the author achieved a certain amount of this goal, this study has some limitations. This study mainly focused on the chemical receptor-motivated sensory system rather than the visuochemical system. However, further research on the utility of this device is required. However, the author claims that visual imaging methods in conjunction with chemical sensors may assist in diagnosing skin disorders or in examining biological samples to identify biomarkers linked to different medical illnesses. Overall, for academics considering their studies in the field of biologically motivated multisensory systems, this literature can be a good motivation.

5.2. Spider web-inspired neurotransmitters

Spiders have a unique method for detecting object motion and airflow and identifying potential threats.[270–272] They use a network of slits known as ''lyriform organs'' that are closely linked to their nervous system, allowing them to pick up external vibrations.[273,274] Additionally, spider viscid silk is known for its remarkable strength, hardness, and adhesiveness, making it an effective tool for prey trapping.[275,276] Spiders regulate the electrostatic connections between spidroin molecular chains by exchanging ions and protons in the spinning duct.[277] This process gives them remarkable mechanical properties, the ability to adhere to surfaces, and the ability to spin silk continuously.

Zhou *et al.* examined artificial spider silk with excellent mechanical characteristics and a conductive structure that facilitated signal transmission (Fig. 13A and B).[278] They used PrDA hydrogel fibers, whose diameter can be easily adjusted by

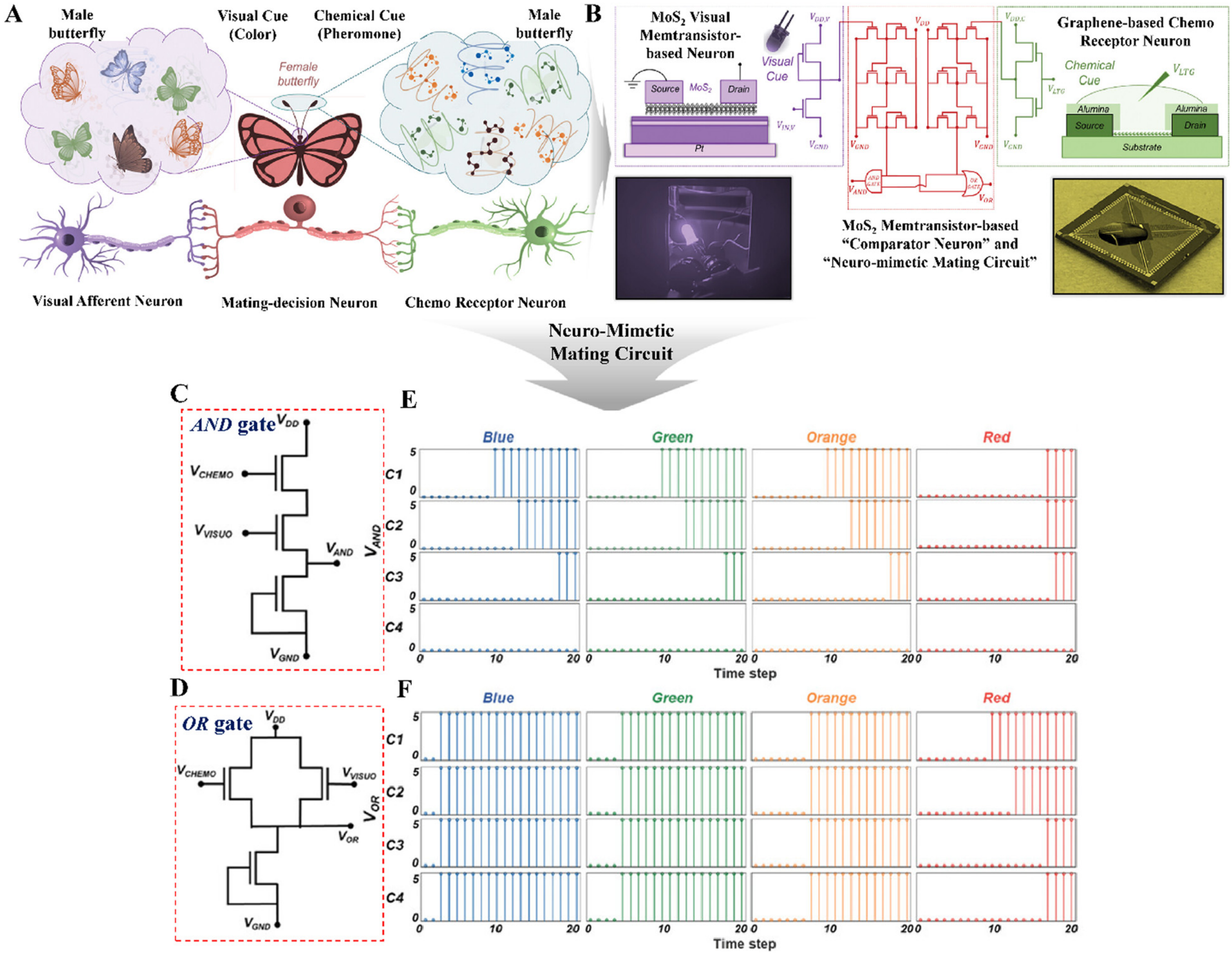

Fig. 12 (A) Visual and chemical signals of a male butterfly interacting with a female butterfly. (B) Optical afferent neurons constructed using MoS_2 memtransistors, chemoreceptor neurons depending on graphene, and breeding pathways relying on MoS_2 memtransistors. Logic circuit. (C) AND gate. (D) OR gate. Four different chemical signals. (E) AND gate. (F) OR gate. Reproduced with permission from ref. 269. Copyright 2023, Wiley-VCH.

controlling the spinning speed and distance between the nozzle and roller (Fig. 13C). Using these fibers, the authors created a synthetic synaptic transistor (Fig. 13E) that imitates the properties of biological synapses (Fig. 13D).

The ability of this transistor to function as a synaptic device was demonstrated using various types (varying diameters) of PrDA fibers, which showed a consistent counterclockwise hysteresis (Fig. 13F). The excitatory postsynaptic potential (EPSC) was distinguishable by different current spikes with varying pulse numbers (Fig. 13G). In addition, as the pulse width increased, the EPSC gradually increased. This trend suggests that a longer duration caused more ions to migrate between the PrDA and In_2O_3 (Indium(III) oxide) layers (Fig. 13H). The paired-pulse facilitation (PPF) index, which is important for signal processing, was higher with a larger gate voltage (Vg) (Fig. 13I), possibly because of the more significant proportion of transferred ions in the active region of the devices, such as biological synapses.

Research on ionic hydrogels as synaptic devices offers a fresh perspective on building artificial neural systems, and this review highlights several promising avenues for further study in this area. Nevertheless, to accomplish a remarkable amalgamation of electromechanics predicted for continuous spinning, further discourse is required concerning obstacles such as interactions between molecules and the hierarchical arrangement of synthetic fibers.

6. Research gaps and future perspectives

This review offers an in-depth overview of the most recent developments in neuromorphic devices inspired by biological synaptic neural systems, keeping in mind the general audience and experts involved in neuromorphic device research. First, we explain how the researchers were motivated by the biological synapse system and then further discuss the neural networks used for single and multi-sensory systems and their advantages and limitations for various applications. Neural networks offer a range of powerful new approaches for addressing complex problems related to pattern recognition, data processing, and control.[279,280] Computer vision, particularly ANNs and CNNs, has become more prevalent as a computational model in neuroscience. However, the intricate neural signals in current models may only partially reveal the enigmas of the brain,[281] for example, (a) the type of code required for real-time transmission of milliseconds of response in terms of voltage spikes, and (b) depending on the human mood, such as anger, the type of signal the brain transmits to control human emotions. Interpreting and understanding intricate patterns may be challenging when using manually created models that prioritize simplicity. Furthermore, object categorization in the brain involves several levels of intricate linear and non-linear processing.[282] Constructing operational models of visual pathways that match human behavioral performance has been a significant issue for neuroscientists and AI researchers.

Nevertheless, neural networks provide significant potential for future researchers by using extensive annotated imaging data for training to create prediction models that can increase output accuracy. Supervised learning is successful because of the detailed feedback provided to the network in the form of high-dimensional outcomes. For example, a model can be trained to determine the lowest price among 10 fruits, depending on seasonal availability. In supervised learning, the same algorithms may be used to predict the lowest price for the 10 other sets of fruits under similar conditions. Some studies have also suggested that convolutional topology and activity

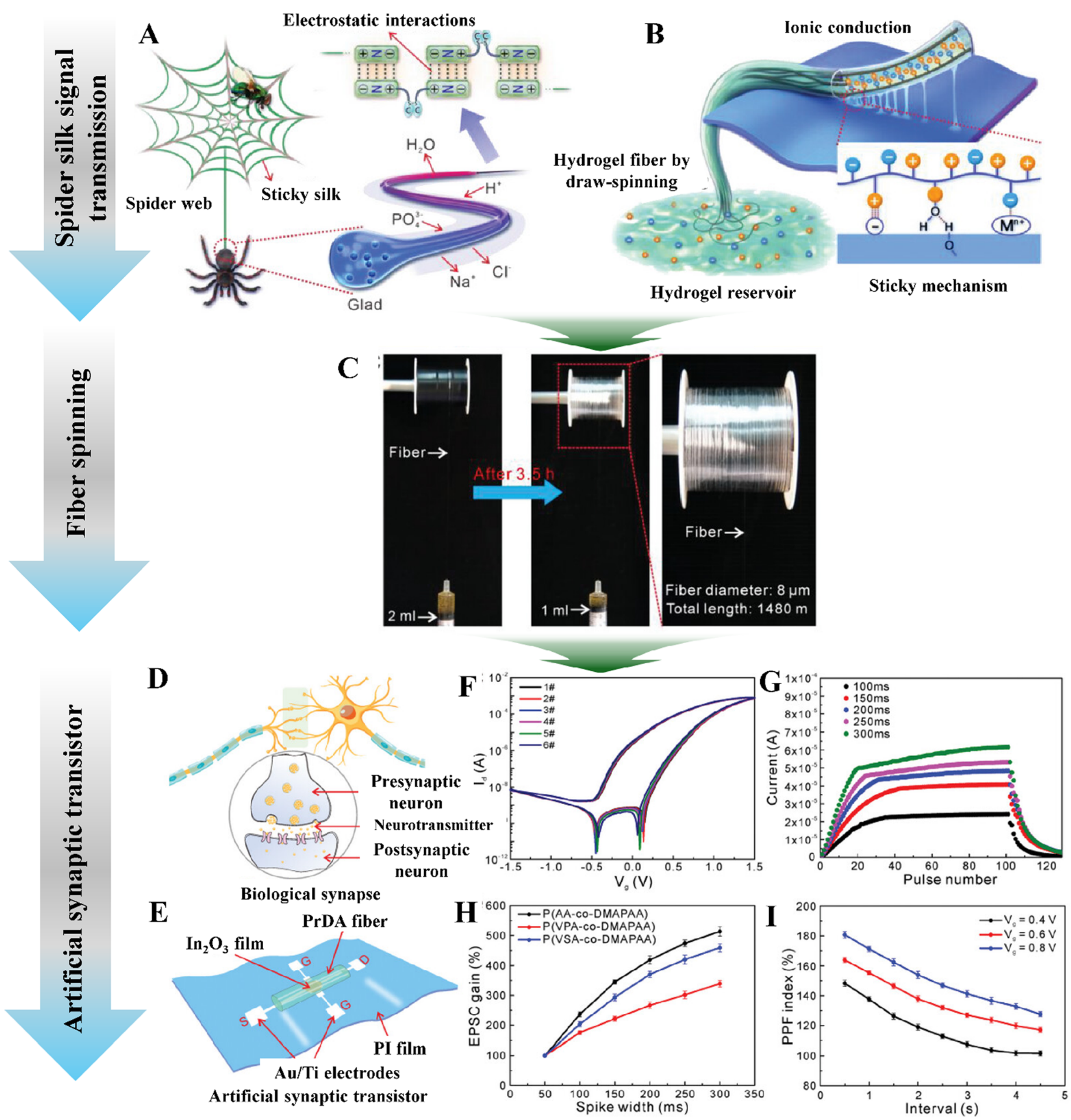

Fig. 13 (A) Electrostatic interaction of a spider web in the spinning duct. (B) Ion transfer and surface adhesion, illustrating the PrDA hydrogel fiber. (C) Continuous draw-spinning of PrDA hydrogel fiber. Synaptic system. (D) Biological synapse. (E) Artificial synaptic transistor. (F) Consistent synaptic transmission properties of the artificial transistor-based on drain-source voltage. (G) EPSC initiated by various voltage pulses from presynaptic spikes. (H) EPSC increases relative to spike width. (I) The PPF index varies across various gate voltages. Reproduced with permission from ref. 278. Copyright 2023, Wiley-VCH.

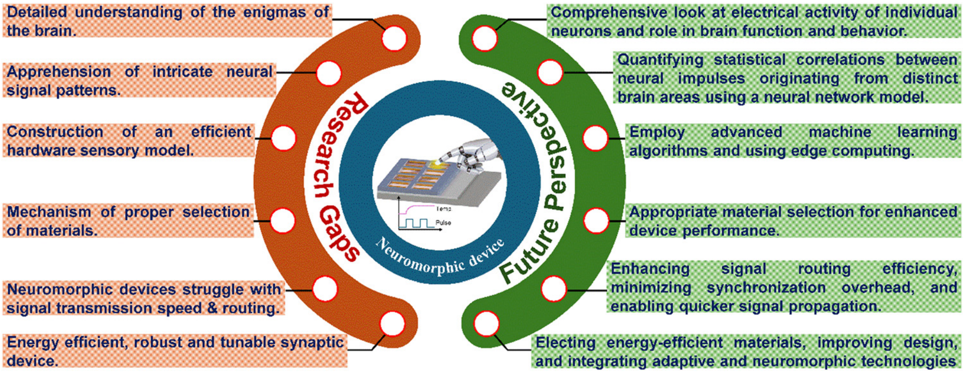

Fig. 14 Research gaps that exist in the recently developed neuromorphic devices.

normalization may result in a well-performing neural model.[283,284] Therefore, the aforementioned learning models should be tested to achieve multidimensional efficient devices.

Artificial synaptic transistors (AST) such as spike-based memristors and neurodevices inspired by the retina are among the artificial synaptic devices covered in this review. Artificial synaptic transistors can closely mimic natural neuromorphic design architectures by considering the timing of the firing action between two neurons (pre- and postsynaptic neurons) as a critical factor affecting the synaptic matrix. Furthermore, there is a consistent need for energy-efficient AST that replicate the functions of neurons and synapses. Neurons interact *via* ion channels,[285,286] which affect their firing rate, which is linked to the intensity of the input stimuli. Increased muscle stimulation leads to a higher neuronal firing rate. The spike frequency activates the synaptic transistor, converting its varying output current into voltage signals to produce the final output. Hence, a highly efficient and consolidated artificial spiking neurological system, such as a medical nanobot, is required to convert the sensing signals into spikes. In addition, signal propagation speed and effective communication routing are issues with spike-based neuromorphic devices.

Artificial synaptic sensors based on the human retina aim to emulate mammalian retinal synaptic neuromorphic sensory systems. Optical artificial synaptic devices consist of two distinct components: photosensors and transistor synaptic devices, each serving specific tasks. These devices have intricate architectures and require additional power to adjust the emanating photosynaptic signals, leading to increased energy consumption and reduced resemblance to biological receptors. Hence, it is essential to create a visual artificial synaptic device using a basic resistor structure that can function autonomously without requiring external power.

The performance of a neuromorphic device is influenced not only by the appropriate selection of an algorithm and a suitable number of training models but also by the selection of appropriate materials for device construction. Researchers have experimented with various material combinations including organic/inorganic materials, metal oxides, semiconductor materials, carbon derivatives, and QDs to develop neuromorphic chips containing artificial synapses. The aim of these chips is to create a brain-like neuromorphic computing system that closely imitates the functions of the human brain. Nevertheless, organic semiconductors exhibit instability at ambient temperatures. Carbon derivatives have restricted speed, integration complexity, and dependence on electrical stimulation, whereas metallic oxides have restricted control and adjustability in neuromorphic activities. Moreover, oxide semiconductors have wide optical bandgaps and low absorption coefficients in the visible light spectrum. Fig. 14 presents a detailed summary of the research gaps and future perspective in the field of neuromorphic systems.

In the future, researchers should focus on developing contemporary neural networks that use neuromorphic computing to address algorithmic issues. Algorithms can affect the design and material selection of hardware layouts for tunable devices that satisfy specific application requirements. Researchers must change their programming approach to optimize the use of neuromorphic computers. Combining suitable materials and architectures with better optical and electrical properties for synaptic devices is possible by learning about synaptic technologies and heterojunction devices that satisfy specific requirements. Considering these minor but impactful steps, researchers can enhance the system performance multiple times. Finally, experts from various fields must collaborate to develop state-of-the-art devices, architectures, and algorithms to create intelligent machines for sensory processing, cognitive science, nanobots, and brain-computer interfaces.

7. Conclusion

Herein, we aim to inform researchers about newly developed neuromorphic devices and their potential future real-world applications. To move from exploratory research to the systematic selection and improvement of the most viable options in neuroscience, researchers must have a comprehensive understanding of the integration of device manufacturing with AI. Embracing new ideas in neuromorphic computing is essential for fully utilizing nanotechnology in neuromorphic systems and devices and for gaining extraordinary insight into the physiology of the human brain, driven by the rapidly expanding body of neuroscience research. We present the learning rules and algorithms used in the neuromorphic systems. Additionally, future research should focus on spike-based neurosystems that are currently trending. Finally, creating engineering approaches that stimulate inherent developmental processes is essential for addressing the challenges mentioned above, although success is not guaranteed. Nevertheless, one can overcome the limitations of neuromorphic science and engineering by aiming for a more positive approach.

Ethical approval

This article does not include any studies with human participants or animals performed by any of the authors.

Consent of publication

All authors provided consent for publication.

Data availability

No primary research results, software or code have been included and no new data were generated or analysed as part of this review.

Conflicts of interest

The authors declare no competing interests.

Acknowledgements

Hongyun So is grateful for financial support from the National Research Foundation of Korea (NRF), funded by the Ministry of Science and ICT of the Republic of Korea (No. NRF- RS-2024-00359316 and RS-2023-00260527).

References

1 S. H. Woolf, D. A. Chapman, J. H. Lee, K. C. Johnston, R. T. Benson, E. Trevathan, W. R. Smith and D. J. Gaskin, *Neurology*, 2023, **101**, 9–16.
2 V. L. Feigin, T. Vos, E. Nichols, M. O. Owolabi, W. M. Carroll, M. Dichgans, G. Deuschl, P. Parmar, M. Brainin and C. Murray, *Lancet Neurol.*, 2020, **19**, 255–265.
3 R. Murrell, *Neuropsychol. Rev.*, 1999, **9**, 209–229.
4 M. Jakovcevski and S. Akbarian, *Nat. Med.*, 2012, **18**, 1194–1204.
5 R. S. Klein, C. Garber and N. Howard, *Nat. Immunol.*, 2017, **18**, 132–141.
6 N. K. Upadhyay, H. Jiang, Z. Wang, S. Asapu, Q. Xia and J. Joshua Yang, *Adv. Mater. Technol.*, 2019, **4**, 1800589.
7 C. D. Schuman, S. R. Kulkarni, M. Parsa, J. P. Mitchell, P. Date and B. Kay, *Nat. Comput. Sci.*, 2022, **2**, 10–19.
8 D. Marković, A. Mizrahi, D. Querlioz and J. Grollier, *Nat. Rev. Phys.*, 2020, **2**, 499–510.
9 Y. van de Burgt, A. Melianas, S. T. Keene, G. Malliaras and A. Salleo, *Nat. Electron.*, 2018, **1**, 386–397.
10 G. W. Burr, R. M. Shelby, A. Sebastian, S. Kim, S. Kim, S. Sidler, K. Virwani, M. Ishii, P. Narayanan, A. Fumarola, L. L. Sanches, I. Boybat, M. Le Gallo, K. Moon, J. Woo, H. Hwang and Y. Leblebici, *Adv. Phys.: X*, 2017, **2**, 89–124.
11 K. Roy, A. Jaiswal and P. Panda, *Nature*, 2019, **575**, 607–617.
12 B. J. Shastri, A. N. Tait, T. Ferreira de Lima, W. H. P. Pernice, H. Bhaskaran, C. D. Wright and P. R. Prucnal, *Nat. Photonics*, 2021, **15**, 102–114.
13 S. Yang, J. Wang, X. Hao, H. Li, X. Wei, B. Deng and K. A. Loparo, *IEEE Trans. Neural Networks. Learn. Syst.*, 2022, **33**, 2801–2815.
14 E. R. Kandel, *Science*, 2001, **294**, 1030–1038.
15 Y. van de Burgt, E. Lubberman, E. J. Fuller, S. T. Keene, G. C. Faria, S. Agarwal, M. J. Marinella, A. Alec Talin and A. Salleo, *Nat. Mater.*, 2017, **16**, 414–418.
16 J. Y. Gerasimov, R. Gabrielsson, R. Forchheimer, E. Stavrinidou, D. T. Simon, M. Berggren and S. Fabiano, *Adv. Sci.*, 2019, **6**, 1801339.
17 D. T. Duong, Y. Tuchman, P. Chakthranont, P. Cavassin, R. Colucci, T. F. Jaramillo, A. Salleo and G. C. Faria, *Adv. Electron. Mater.*, 2018, **4**, 1800090.
18 S. Lee, Y. W. Cho, J. Lee, Y. Jung, S. Oh, J. Sun, S. Kim and Y. Joo, *Adv. Sci.*, 2021, **8**, 2001544.
19 Y. Zhang, G. Ye, T. P. A. van der Pol, J. Dong, E. R. W. van Doremaele, I. Krauhausen, Y. Liu, P. Gkoupidenis, G. Portale, J. Song, R. C. Chiechi and Y. van de Burgt, *Adv. Funct. Mater.*, 2022, **32**, 2201593.
20 K. Janzakova, M. Ghazal, A. Kumar, Y. Coffinier, S. Pecqueur and F. Alibart, *Adv. Sci.*, 2021, **8**, 2102973.
21 M. A. Zidan, J. P. Strachan and W. D. Lu, *Nat. Electron.*, 2018, **1**, 22–29.
22 M. Prezioso, F. Merrikh-Bayat, B. D. Hoskins, G. C. Adam, K. K. Likharev and D. B. Strukov, *Nature*, 2015, **521**, 61–64.
23 Z. Wang, S. Joshi, S. E. Savel'ev, H. Jiang, R. Midya, P. Lin, M. Hu, N. Ge, J. P. Strachan, Z. Li, Q. Wu, M. Barnell, G.-L. Li, H. L. Xin, R. S. Williams, Q. Xia and J. J. Yang, *Nat. Mater.*, 2017, **16**, 101–108.
24 S. Kumar, X. Wang, J. P. Strachan, Y. Yang and W. D. Lu, *Nat. Rev. Mater.*, 2022, **7**, 575–591.
25 X. Duan, Z. Cao, K. Gao, W. Yan, S. Sun, G. Zhou, Z. Wu, F. Ren and B. Sun, *Adv. Mater.*, 2024, 202310704.
26 Y. Lee, Y. Liu, D.-G. Seo, J. Y. Oh, Y. Kim, J. Li, J. Kang, J. Kim, J. Mun, A. M. Foudeh, Z. Bao and T.-W. Lee, *Nat. Biomed. Eng.*, 2022, **7**, 511–519.
27 Y. Kim, A. Chortos, W. Xu, Y. Liu, J. Y. Oh, D. Son, J. Kang, A. M. Foudeh, C. Zhu, Y. Lee, S. Niu, J. Liu, R. Pfattner, Z. Bao and T.-W. Lee, *Science*, 2018, **360**, 998–1003.
28 H. Wei, R. Shi, L. Sun, H. Yu, J. Gong, C. Liu, Z. Xu, Y. Ni, J. Xu and W. Xu, *Nat. Commun.*, 2021, **12**, 1068.
29 Y. Wang, Y. Zhu, Y. Li, Y. Zhang, D. Yang and X. Pi, *Adv. Funct. Mater.*, 2022, 2107973.

30 Q. Wan, M. T. Sharbati, J. R. Erickson, Y. Du and F. Xiong, *Adv. Mater. Technol.*, 2019, **4**, 1900037.
31 S. Zhao, Z. Ni, H. Tan, Y. Wang, H. Jin, T. Nie, M. Xu, X. Pi and D. Yang, *Nano Energy*, 2018, **54**, 383–389.
32 G. Cao, P. Meng, J. Chen, H. Liu, R. Bian, C. Zhu, F. Liu and Z. Liu, *Adv. Funct. Mater.*, 2021, **31**, 2005443.
33 L. Sun, W. Wang and H. Yang, *Adv. Intell. Syst.*, 2020, **2**, 1900167.
34 H. Tian, X. Cao, Y. Xie, X. Yan, A. Kostelec, D. DiMarzio, C. Chang, L.-D. Zhao, W. Wu, J. Tice, J. J. Cha, J. Guo and H. Wang, *ACS Nano*, 2017, **11**, 7156–7163.
35 Y. Wang, L. Yin, W. Huang, Y. Li, S. Huang, Y. Zhu, D. Yang and X. Pi, *Adv. Intell. Syst.*, 2020, **3**, 2000099.
36 P. A. Merolla, J. V. Arthur, B. E. Shi and K. A. Boahen, *IEEE Trans. Circuits Syst.*, 2007, **54**, 301–311.
37 K. A. Zaghloul and K. Boahen, *IEEE Trans. Biomed. Eng.*, 2004, **51**, 667–675.
38 K. A. Boahen, *IEEE Trans. Circuits Syst.*, 2000, **47**, 416–434.
39 K. Byun, I. Choi, S. Kwon, Y. Kim, D. Kang, Y. W. Cho, S. K. Yoon and S. Kim, *Adv. Mater. Technol.*, 2023, **8**, 2200884.
40 I. Krauhausen, D. A. Koutsouras, A. Melianas, S. T. Keene, K. Lieberth, H. Ledanseur, R. Sheelamanthula, A. Giovannitti, F. Torricelli, I. Mcculloch, P. W. M. Blom, A. Salleo, Y. van de Burgt and P. Gkoupidenis, *Sci. Adv.*, 2021, **7**, 50.
41 T. Hwu, J. Isbell, N. Oros and J. Krichmar, *Int. Jt. Conf. Neural Networks*, 2017, 635–641.
42 H. Park, Y. Lee, N. Kim, D. Seo, G. Go and T. Lee, *Adv. Mater.*, 2020, **32**, 1903558.
43 A. D. Rast, S. V. Adams, S. Davidson, S. Davies, M. Hopkins, A. Rowley, A. B. Stokes, T. Wennekers, S. Furber and A. Cangelosi, *IEEE Trans. Neural Networks. Learn. Syst.*, 2018, **29**, 6132–6144.
44 H. Chiroma, U. A. Abdullahi, S. M. Abdulhamid, A. Abdulsalam Alarood, L. A. Gabralla, N. Rana, L. Shuib, I. A. Targio Hashem, D. E. Gbenga, A. I. Abubakar, A. M. Zeki and T. Herawan, *IEEE Access*, 2019, **7**, 70535–70551.
45 H. Yu, H. Wei, J. Gong, H. Han, M. Ma, Y. Wang and W. Xu, *Small*, 2021, **17**, 2000041.
46 P. C. Harikesh, C.-Y. Yang, D. Tu, J. Y. Gerasimov, A. M. Dar, A. Armada-Moreira, M. Massetti, R. Kroon, D. Bliman, R. Olsson, E. Stavrinidou, M. Berggren and S. Fabiano, *Nat. Commun.*, 2022, **13**, 901.
47 A. H. Atabaki, S. Moazeni, F. Pavanello, H. Gevorgyan, J. Notaros, L. Alloatti, M. T. Wade, C. Sun, S. A. Kruger, H. Meng, K. Al Qubaisi, I. Wang, B. Zhang, A. Khilo, C. V. Baiocco, M. A. Popović, V. M. Stojanović and R. J. Ram, *Nature*, 2018, **556**, 349–354.
48 M. M. Shulaker, G. Hills, R. S. Park, R. T. Howe, K. Saraswat, H.-S. P. Wong and S. Mitra, *Nature*, 2017, **547**, 74–78.
49 K. Y. Camsari, R. Faria, B. M. Sutton and S. Datta, *Phys. Rev. X*, 2017, **7**, 031014.
50 W. C. Stacey, *EBioMedicine*, 2018, **27**, 3–4.
51 I. Kiral-Kornek, S. Roy, E. Nurse, B. Mashford, P. Karoly, T. Carroll, D. Payne, S. Saha, S. Baldassano, T. O'Brien, D. Grayden, M. Cook, D. Freestone and S. Harrer, *EBioMedicine*, 2018, **27**, 103–111.
52 A. Dorzhigulov and V. Saxena, *Front. Neurosci.*, 2023, **17**, 1177592.
53 N. Gong, T. Idé, S. Kim, I. Boybat, A. Sebastian, V. Narayanan and T. Ando, *Nat. Commun.*, 2018, **9**, 2102.
54 M. Naqi, Y. Cho, A. Bala and S. Kim, *Mater. Today Electron.*, 2023, **5**, 100052.
55 Y. Fathy, P. Barnaghi and R. Tafazolli, *IEEE Syst. J.*, 2019, **13**, 2688–2699.
56 U. Satija, B. Ramkumar and M. S. Manikandan, *IEEE Rev. Biomed. Eng.*, 2018, **11**, 36–52.
57 A. Amedi, K. von Kriegstein, N. M. van Atteveldt, M. S. Beauchamp and M. J. Naumer, *Exp. Brain Res.*, 2005, **166**, 559–571.
58 S. Molholm, *Cereb. Cortex*, 2004, **14**, 452–465.
59 F. Zhou, Z. Zhou, J. Chen, T. H. Choy, J. Wang, N. Zhang, Z. Lin, S. Yu, J. Kang, H.-S. P. Wong and Y. Chai, *Nat. Nanotechnol.*, 2019, **14**, 776–782.
60 S. Park, Y. Jeong, H.-J. Jin, J. Park, H. Jang, S. Lee, W. Huh, H. Cho, H. G. Shin, K. Kim, C.-H. Lee, S. Choi and S. Im, *ACS Nano*, 2020, **14**, 12064–12071.
61 H. Shim, S. Jang, A. Thukral, S. Jeong, H. Jo, B. Kan, S. Patel, G. Wei, W. Lan, H.-J. Kim and C. Yu, *Proc. Natl. Acad. Sci. U. S. A.*, 2022, **119**, e2204852119.
62 Y. Guo, F. Wu, G. Dun, T. Cui, Y. Liu, X. Tan, Y. Qiao, M. Lanza, H. Tian, Y. Yang and T. Ren, *Adv. Funct. Mater.*, 2023, **33**, 2208055.
63 A. Peters and S. L. Palay, *J. Neurocytol.*, 1996, **25**, 687–700.
64 A. E. Pereda, *Nat. Rev. Neurosci.*, 2014, **15**, 250–263.
65 T. C. Südhof, *J. Cell Biol.*, 2021, **7**, 220.
66 S. Nakanishi, *Science*, 1992, **258**, 597–603.
67 A. Avila, L. Nguyen and J.-M. Rigo, *Front. Cell. Neurosci.*, 2013, **7**, 184.
68 T.-S. Wong, G. Li, S. Li, W. Gao, G. Chen, S. Gan, M. Zhang, H. Li, S. Wu and Y. Du, *Signal Transduction Targeted Ther.*, 2023, **8**, 177.
69 C. Zhu, H. Liu, W. Wang, L. Xiang, J. Jiang, Q. Shuai, X. Yang, T. Zhang, B. Zheng, H. Wang, D. Li and A. Pan, *Light: Sci. Appl.*, 2022, **11**, 337.
70 A. J. Arnold, A. Razavieh, J. R. Nasr, D. S. Schulman, C. M. Eichfeld and S. Das, *ACS Nano*, 2017, **11**, 3110–3118.
71 A. Dani, B. Huang, J. Bergan, C. Dulac and X. Zhuang, *Neuron*, 2010, **68**, 843–856.
72 C. P. Taylor and F. E. Dudek, *Science*, 1982, **218**, 810–812.
73 C. E. Landisman and B. W. Connors, *Science*, 2005, **310**, 1809–1813.
74 D. Guo, Q. Wang and M. Perc, *Phys. Rev. E: Stat., Nonlinear, Soft Matter Phys.*, 2012, **85**, 061905.
75 M. Galarreta and S. Hestrin, *Nature*, 1999, **402**, 72–75.
76 M. F. Johnston, S. A. Simon and F. Ramón, *Nature*, 1980, **286**, 498–500.
77 J. S. Haas, B. Zavala and C. E. Landisman, *Science*, 2011, **334**, 389–393.

78 H. Roh, S. Yue, H. Hu, K. Chen, H. J. Kulik and A. Gumyusenge, *Adv. Funct. Mater.*, 2023, **33**, 2304893.

79 H. Wang, Q. Zhao, Z. Ni, Q. Li, H. Liu, Y. Yang, L. Wang, Y. Ran, Y. Guo, W. Hu and Y. Liu, *Adv. Mater.*, 2018, **30**, 1803961.

80 J. Ji, Z. Wang, F. Zhang, B. Wang, Y. Niu, X. Jiang, Z. Qiao, T. Ren, W. Zhang, S. Sang, Z. Cheng and Q. Sun, *InfoMat*, 2023, **5**, 11.

81 X. Li, R. Bi, X. Ou, S. Han, Y. Sheng, G. Chen, Z. Xie, C. Liu, W. Yue, Y. Wang, W. Hu and S.-Z. Guo, *ACS Appl. Mater. Interfaces*, 2023, **15**, 41656–41665.

82 Z. Cheng, C. Ríos, W. H. P. Pernice, C. D. Wright and H. Bhaskaran, *Sci. Adv.*, 2017, **3**, e1700160.

83 H. Park, H. Kim, D. Lim, H. Zhou, Y. Kim, Y. Lee, S. Park and T. Lee, *Adv. Mater.*, 2020, **32**, 1906899.

84 T. Chen, X. Wang, D. Hao, S. Dai, Q. Ou, J. Zhang and J. Huang, *Adv. Opt. Mater.*, 2021, **9**, 2002030.

85 S. Wang, H. Chen, T. Liu, Y. Wei, G. Yao, Q. Lin, X. Han, C. Zhang and H. Huang, *Angew. Chem.*, 2023, **135**, e202213733.

86 H. H. Chouhdry, D. H. Lee, A. Bag and N.-E. Lee, *Nat. Commun.*, 2023, **14**, 821.

87 M. Shin, Y. Wang, J. R. Borgus and B. J. Venton, *Annu. Rev. Anal. Chem.*, 2019, **12**, 297–321.

88 X. Yao, K. Klyukin, W. Lu, M. Onen, S. Ryu, D. Kim, N. Emond, I. Waluyo, A. Hunt, J. A. del Alamo, J. Li and B. Yildiz, *Nat. Commun.*, 2020, **11**, 3134.

89 T. C. Südhof, *Neuron*, 2018, **100**, 276–293.

90 C. Qian, J. Sun, L. Kong, G. Gou, J. Yang, J. He, Y. Gao and Q. Wan, *ACS Appl. Mater. Interfaces*, 2016, **8**, 26169–26175.

91 M. Huang, M. Schwacke, M. Onen, J. del Alamo, J. Li and B. Yildiz, *Adv. Mater.*, 2023, **35**, 2205169.

92 S. Chen, T. Zhang, S. Tappertzhofen, Y. Yang and I. Valov, *Adv. Mater.*, 2023, **35**, 2301924.

93 R. Bhunia, E. K. Boahen, D. J. Kim, H. Oh, Z. Kong and D. H. Kim, *J. Mater. Chem. C*, 2023, **11**, 7485–7509.

94 Y. Shen, A. R. Hosseini, M. H. Wong and G. G. Malliaras, *Chem. Phys. Chem.*, 2004, **5**, 16–25.

95 Q. Wu, J. Wang, J. Cao, C. Lu, G. Yang, X. Shi, X. Chuai, Y. Gong, Y. Su, Y. Zhao, N. Lu, D. Geng, H. Wang, L. Li and M. Liu, *Adv. Electron. Mater.*, 2018, **4**, 1800556.

96 M. Lee, W. Lee, S. Choi, J. Jo, J. Kim, S. K. Park and Y. Kim, *Adv. Mater.*, 2017, **29**, 1700951.

97 X. Zhu and W. D. Lu, *ACS Nano*, 2018, **12**, 1242–1249.

98 R. A. John, F. Liu, N. A. Chien, M. R. Kulkarni, C. Zhu, Q. Fu, A. Basu, Z. Liu and N. Mathews, *Adv. Mater.*, 2018, **30**, 1800220.

99 S. Ham, S. Choi, H. Cho, S. Na and G. Wang, *Adv. Funct. Mater.*, 2019, **29**, 1806646.

100 K. Wang, S. Dai, Y. Zhao, Y. Wang, C. Liu and J. Huang, *Small*, 2019, **15**, 1900010.

101 K. He, Y. Liu, J. Yu, X. Guo, M. Wang, L. Zhang, C. Wan, T. Wang, C. Zhou and X. Chen, *ACS Nano*, 2022, **16**, 9691–9700.

102 Y. Wang, Y. Zha, C. Bao, F. Hu, Y. Di, C. Liu, F. Xing, X. Xu, X. Wen, Z. Gan and B. Jia, *Adv. Mater.*, 2024, 2311524.

103 L. Gu, Y. Li, D. Xie and J. Jiang, *IEEE Trans. Electron Devices*, 2022, **69**, 4382–4385.

104 X. Wang, Y. Yan, E. Li, Y. Liu, D. Lai, Z. Lin, Y. Liu, H. Chen and T. Guo, *Nano Energy*, 2020, **75**, 104952.

105 S. M. Kwon, S.-H. Kang, S. S. Cho, Y.-W. Jang, S.-J. Nam, J. Kim, U.-C. Moon, J.-W. Shin, Y.-H. Kim and S. K. Park, *ACS Appl. Electron. Mater.*, 2022, **4**, 2629–2635.

106 M. Karbalaei Akbari, R. K. Ramachandran, C. Detavernier, J. Hu, J. Kim, F. Verpoort and S. Zhuiykov, *J. Mater. Chem. C*, 2021, **9**, 2539–2549.

107 M. D. Godfrey and D. F. Hendry, *IEEE Ann. Hist. Comput.*, 1993, **15**, 11–21.

108 S. Kim, H. Kim, S. Hwang, M.-H. Kim, Y.-F. Chang and B.-G. Park, *ACS Appl. Mater. Interfaces*, 2017, **9**, 40420–40427.

109 J. J. Seoane, J. Parra, J. Navarro-Arenas and P. Sanchis, *Opt. Mater. Express*, 2023, **13**, 3266.

110 H. Dong, X. Zheng, C. Cheng, L. Qian, Y. Cui, W. Wu, Q. Liu, X. Chen, Y. Lu, Q. Yang, F. Zhang and D. Wang, *Adv. Sci.*, 2023, **10**, 2206699.

111 K. J. Kwak, J. H. Baek, D. E. Lee, I. Hyuk Im, J. Kim, S. J. Kim, Y. J. Lee, J. Y. Kim and H. W. Jang, *Nano Lett.*, 2022, **22**, 6010–6017.

112 E. Raza, F. Aziz and Z. Ahmad, *RSC Adv.*, 2018, **8**, 20952–20967.

113 W. Xu, H. Cho, Y. Kim, Y. Kim, C. Wolf, C. Park and T. Lee, *Adv. Mater.*, 2016, **28**, 5916–5922.

114 W. Tan, A. R. Bowring, A. C. Meng, M. D. McGehee and P. C. McIntyre, *ACS Appl. Mater. Interfaces*, 2018, **10**, 5485–5491.

115 P. Qin, S. Tanaka, S. Ito, N. Tetreault, K. Manabe, H. Nishino, M. K. Nazeeruddin and M. Grätzel, *Nat. Commun.*, 2014, **5**, 3834.

116 K. Galkowski, A. Surrente, M. Baranowski, B. Zhao, Z. Yang, A. Sadhanala, S. Mackowski, S. D. Stranks and P. Plochocka, *ACS Energy Lett.*, 2019, **4**, 615–621.

117 O. A. Jaramillo-Quintero, M. Solís de la Fuente, R. S. Sanchez, I. B. Recalde, E. J. Juarez-Perez, M. E. Rincón and I. Mora-Seró, *Nanoscale*, 2016, **8**, 6271–6277.

118 G. Vats, B. Hodges, A. J. Ferguson, L. M. Wheeler and J. L. Blackburn, *Adv. Mater.*, 2023, **35**, 202205459.

119 H. Lee, Y. Won and J. H. Oh, *J. Polym. Sci.*, 2022, **60**, 348–376.

120 J. Y. Kwon, J. E. Kim, J. S. Kim, S. Y. Chun, K. Soh and J. H. Yoon, *Exploration*, 2024, **4**, 20220162.

121 S. R. Forrest, *Nature*, 2004, **428**, 911–918.

122 R. Bhunia, J. S. Kim, H. Kweon, D. J. Kim and D. H. Kim, *Mater. Chem. Phys.*, 2022, **287**, 126227.

123 M. Di Lauro, A. De Salvo, G. C. Sebastianella, M. Bianchi, S. Carli, M. Murgia, L. Fadiga and F. Biscarini, *ACS Appl. Electron. Mater.*, 2020, **2**, 1849–1854.

124 K. Janzakova, I. Balafrej, A. Kumar, N. Garg, C. Scholaert, J. Rouat, D. Drouin, Y. Coffinier, S. Pecqueur and F. Alibart, *Nat. Commun.*, 2023, **14**, 8143.

125 S. Oh, H. Kim, S. E. Kim, M.-H. Kim, H.-L. Park and S.-H. Lee, *Adv. Intell. Syst.*, 2023, **5**, 2200272.

126 W. Xu, S.-Y. Min, H. Hwang and T.-W. Lee, *Sci. Adv.*, 2016, **2**, e1501326.
127 M. M. H. Tanim, Z. Templin, K. Hood, J. Jiao and F. Zhao, *Adv. Mater. Technol.*, 2023, **8**, 2202194.
128 Q. Lin, Z. Wang, M. Young, J. B. Patel, R. L. Milot, L. Martinez Maestro, R. R. Lunt, H. J. Snaith, M. B. Johnston and L. M. Herz, *Adv. Funct. Mater.*, 2017, **27**, 1702485.
129 X. Li, F. Cao, D. Yu, J. Chen, Z. Sun, Y. Shen, Y. Zhu, L. Wang, Y. Wei, Y. Wu and H. Zeng, *Small*, 2017, **13**, 1603996.
130 Q. Tian, R. Hong, C. Liu, X. Hong, S. Zhang, L. Wang, Y. Lv, X. Liu, X. Zou and L. Liao, *Nano Lett.*, 2022, **22**, 494–500.
131 J. Choi, J. S. Han, K. Hong, S. Y. Kim and H. W. Jang, *Adv. Mater.*, 2018, **30**, 1704002.
132 H. Patil, H. Kim, K. D. Kadam, S. Rehman, S. A. Patil, J. Aziz, T. D. Dongale, Z. Ali Sheikh, M. Khalid Rahmani, M. F. Khan and D. Kim, *ACS Appl. Mater. Interfaces*, 2023, **15**, 13238–13248.
133 G. Feng, J. Jiang, Y. Zhao, S. Wang, B. Liu, K. Yin, D. Niu, X. Li, Y. Chen, H. Duan, J. Yang, J. He, Y. Gao and Q. Wan, *Adv. Mater.*, 2020, **32**, 1906171.
134 T. Q. Trung, A. Bag, L. T. N. Huyen, M. Meeseepong and N. Lee, *Adv. Funct. Mater.*, 2024, **34**, 2309378.
135 C. Zhang, Y. Li, C. Ma and Q. Zhang, *Small Sci.*, 2022, **2**, 2100086.
136 K. Liao, P. Lei, M. Tu, S. Luo, T. Jiang, W. Jie and J. Hao, *ACS Appl. Mater. Interfaces*, 2021, **13**, 32606–32623.
137 C. Ban, Z. Zhang, C. Song, H. Zhang, X. Luo, X. Wang, J. Liu, Z. Liu and W. Huang, *Adv. Mater. Technol.*, 2023, **8**, 2200870.
138 T. Mazur, P. Zawal and K. Szaciłowski, *Nanoscale*, 2019, **11**, 1080–1090.
139 G. Chen, J. Seo, C. Yang and P. N. Prasad, *Chem. Soc. Rev.*, 2013, **42**, 8304.
140 S. Kundu and A. Patra, *Chem. Rev.*, 2017, **117**, 712–757.
141 R. Yu, Q. Lin, S.-F. Leung and Z. Fan, *Nano Energy*, 2012, **1**, 57–72.
142 L. Xu, S. Yuan, H. Zeng and J. Song, *Mater. Today Nano*, 2019, **6**, 100036.
143 J. Ren, T. Li, X. Zhou, X. Dong, A. V. Shorokhov, M. B. Semenov, V. D. Krevchik and Y. Wang, *Chem. Eng. J.*, 2019, **358**, 30–39.
144 S. Yuan, Z.-K. Wang, M.-P. Zhuo, Q.-S. Tian, Y. Jin and L.-S. Liao, *ACS Nano*, 2018, **12**, 9541–9548.
145 W.-C. Chen, Y.-H. Fang, L.-G. Chen, F.-C. Liang, Z.-L. Yan, H. Ebe, Y. Takahashi, T. Chiba, J. Kido and C.-C. Kuo, *Chem. Eng. J.*, 2021, **414**, 128866.
146 S. Akin, Y. Altintas, E. Mutlugun and S. Sonmezoglu, *Nano Energy*, 2019, **60**, 557–566.
147 M. Leng, Y. Yang, K. Zeng, Z. Chen, Z. Tan, S. Li, J. Li, B. Xu, D. Li, M. P. Hautzinger, Y. Fu, T. Zhai, L. Xu, G. Niu, S. Jin and J. Tang, *Adv. Funct. Mater.*, 2018, **28**, 1704446.
148 Y. Wang, Z. Lv, J. Chen, Z. Wang, Y. Zhou, L. Zhou, X. Chen and S. Han, *Adv. Mater.*, 2018, **30**, 1802883.
149 Z. Chen, Q. Dong, Y. Liu, C. Bao, Y. Fang, Y. Lin, S. Tang, Q. Wang, X. Xiao, Y. Bai, Y. Deng and J. Huang, *Nat. Commun.*, 2017, **8**, 1890.
150 D. Hao, J. Zhang, S. Dai, J. Zhang and J. Huang, *ACS Appl. Mater. Interfaces*, 2020, **12**, 39487–39495.
151 J. Chen, D. Yang, F. Jhuang, Y. Fang, J. Benas, F. Liang and C. Kuo, *Adv. Funct. Mater.*, 2021, **31**, 2105911.
152 E. Ercan, Y. Lin, W. Yang and W. Chen, *Adv. Funct. Mater.*, 2022, **32**, 2107925.
153 G. K. Gupta, I.-J. Kim, Y. Park, M.-K. Kim and J.-S. Lee, *ACS Appl. Mater. Interfaces*, 2023, **15**, 18055–18064.
154 Y. R. Park and G. Wang, *Adv. Funct. Mater.*, 2024, **34**, 2307971.
155 U. Jung, J. Lim, S. Kim and J. Park, *J. Alloys Compd.*, 2024, **972**, 172771.
156 P. J. Gemperline, J. R. Long and V. G. Gregoriou, *Anal. Chem.*, 1991, **63**, 2313–2323.
157 M. A. Soriano, F. Khan and R. Ahmad, *IEEE Trans. Instrum. Meas.*, 2020, **69**, 6787–6794.
158 Y. Fang, Y. Zou, J. Xu, G. Chen, Y. Zhou, W. Deng, X. Zhao, M. Roustaei, T. K. Hsiai and J. Chen, *Adv. Mater.*, 2021, **33**, 2104178.
159 Y. Tong, Z. Feng, J. Kim, J. L. Robertson, X. Jia and B. N. Johnson, *Nano Energy*, 2020, **75**, 104973.
160 L. Shu Fang, C. Y. Tsai, M. H. Xu, S. W. Wu, W. C. Lo, Y. H. Lu and Y. K. Fuh, *Nanotechnology*, 2020, **31**, 155502.
161 K. K. Kim, I. Ha, M. Kim, J. Choi, P. Won, S. Jo and S. H. Ko, *Nat. Commun.*, 2020, **11**, 2149.
162 M. Wang, Z. Yan, T. Wang, P. Cai, S. Gao, Y. Zeng, C. Wan, H. Wang, L. Pan, J. Yu, S. Pan, K. He, J. Lu and X. Chen, *Nat. Electron.*, 2020, **3**, 563–570.
163 Y. Fang, J. Xu, X. Xiao, Y. Zou, X. Zhao, Y. Zhou and J. Chen, *Adv. Mater.*, 2022, **34**, 2200252.
164 Y. Qiu, Z. Wang, P. Zhu, B. Su, C. Wei, Y. Tian, Z. Zhang, H. Chai, A. Liu, L. Liang and H. Wu, *Chem. Eng. J.*, 2023, **455**, 140890.
165 M. Liu, Y. Zhang, J. Wang, N. Qin, H. Yang, K. Sun, J. Hao, L. Shu, J. Liu, Q. Chen, P. Zhang and T. H. Tao, *Nat. Commun.*, 2022, **13**, 79.
166 G. Li, S. Liu, L. Wang and R. Zhu, *Sci. Rob.*, 2020, **5**, eabc8134.
167 Z. Sun, M. Zhu, Z. Zhang, Z. Chen, Q. Shi, X. Shan, R. C. H. Yeow and C. Lee, *Adv. Sci.*, 2021, **8**, 2100230.
168 X. Qu, Z. Liu, P. Tan, C. Wang, Y. Liu, H. Feng, D. Luo, Z. Li and Z. L. Wang, *Sci. Adv.*, 2022, **8**, eabq2521.
169 Y. Wang, M. L. Adam, Y. Zhao, W. Zheng, L. Gao, Z. Yin and H. Zhao, *Nano-Micro Lett.*, 2023, **15**, 55.
170 T. Sun, B. Feng, J. Huo, Y. Xiao, W. Wang, J. Peng, Z. Li, C. Du, W. Wang, G. Zou and L. Liu, *Nano-Micro Lett.*, 2024, **16**, 14.
171 J. Xie, Y. Zhao, D. Zhu, J. Yan, J. Li, M. Qiao, G. He and S. Deng, *ACS Appl. Mater. Interfaces*, 2023, **15**, 12551–12559.
172 Z. Gao, Y. Song, T. Y. Hsiao, J. He, C. Wang, J. Shen, A. MacLachlan, S. Dai, B. H. Singer, K. Kurabayashi and P. Chen, *ACS Nano*, 2021, **15**, 18023–18036.
173 S. Wanninger, P. Asadiatouei, J. Bohlen, C.-B. Salem, P. Tinnefeld, E. Ploetz and D. C. Lamb, *Nat. Commun.*, 2023, **14**, 6564.
174 L. Shan, Q. Chen, R. Yu, C. Gao, L. Liu, T. Guo and H. Chen, *Nat. Commun.*, 2023, **14**, 2648.

175 G. Liu, W. Wen, Z. Zhao, X. Huang, Y. Li, M. Qin, Z. Pan, Y. Guo and Y. Liu, *Adv. Mater.*, 2023, **35**, 2300242.
176 H. Wei, G. Yao, Y. Ni, L. Yang, J. Liu, L. Sun, X. Zhang, J. Yang, Y. Xiao, F. Zheng and W. Xu, *Adv. Funct. Mater.*, 2023, **33**, 2304000.
177 X. Wu, E. Li, Y. Liu, W. Lin, R. Yu, G. Chen, Y. Hu, H. Chen and T. Guo, *Nano Energy*, 2021, **85**, 106000.
178 M. Pei, Y. Zhu, S. Liu, H. Cui, Y. Li, Y. Yan, Y. Li, C. Wan and Q. Wan, *Adv. Mater.*, 2023, **35**, 2305609.
179 Y. Sun, J. Li, S. Li, Y. Jiang, E. Wan, J. Zhang, Y. Shi and L. Pan, *Chip*, 2023, **2**, 100031.
180 F. Sun, Q. Lu, S. Feng and T. Zhang, *ACS Nano*, 2021, **15**, 3875–3899.
181 R. Yuan, Q. Duan, P. J. Tiw, G. Li, Z. Xiao, Z. Jing, K. Yang, C. Liu, C. Ge, R. Huang and Y. Yang, *Nat. Commun.*, 2022, **13**, 3973.
182 F. McGlone, J. Wessberg and H. Olausson, *Neuron*, 2014, **82**, 737–755.
183 G. T. Meijer, P. E. C. Mertens, C. M. A. Pennartz, U. Olcese and C. S. Lansink, *Prog. Neurobiol.*, 2019, **174**, 1–15.
184 D. D. Frank, G. C. Jouandet, P. J. Kearney, L. J. Macpherson and M. Gallio, *Nature*, 2015, **519**, 358–361.
185 H. H. Ehrsson, N. P. Holmes and R. E. Passingham, *J. Neurosci.*, 2005, **25**, 10564–10573.
186 G. Gentile, A. Guterstam, C. Brozzoli and H. H. Ehrsson, *J. Neurosci.*, 2013, **33**, 13350–13366.
187 D. Senkowski, D. Saint-Amour, M. Höfle and J. J. Foxe, *NeuroImage*, 2011, **56**, 2200–2208.
188 N. P. Holmes, *Brain Topogr.*, 2009, **21**, 168–176.
189 R. Ratnam and M. E. Nelson, *J. Neurosci.*, 2000, **20**, 6672–6683.
190 J.-K. Han, S.-Y. Yun, J.-M. Yu, S.-B. Jeon and Y.-K. Choi, *ACS Appl. Mater. Interfaces*, 2023, **15**, 5449–5455.
191 G. Liu, Q. Li, W. Shi, Y. Liu, K. Liu, X. Yang, M. Shao, A. Guo, X. Huang, F. Zhang, Z. Zhao, Y. Guo and Y. Liu, *Adv. Funct. Mater.*, 2022, **32**, 2200959.
192 M. U. K. Sadaf, N. U. Sakib, A. Pannone, H. Ravichandran and S. Das, *Nat. Commun.*, 2023, **14**, 5729.
193 J. He, R. Wei, S. Ge, W. Wu, J. Guo, J. Tao, R. Wang, C. Wang and C. Pan, *InfoMat*, 2024, **6**, e12493.
194 J. Zhu, X. Zhang, R. Wang, M. Wang, P. Chen, L. Cheng, Z. Wu, Y. Wang, Q. Liu and M. Liu, *Adv. Mater.*, 2022, **34**, 2200481.
195 L. Liu, W. Xu, Y. Ni, Z. Xu, B. Cui, J. Liu, H. Wei and W. Xu, *ACS Nano*, 2022, **16**, 2282–2291.
196 W. Wang, Y. Jiang, D. Zhong, Z. Zhang, S. Choudhury, J.-C. Lai, H. Gong, S. Niu, X. Yan, Y. Zheng, C.-C. Shih, R. Ning, Q. Lin, D. Li, Y.-H. Kim, J. Kim, Y.-X. Wang, C. Zhao, C. Xu, X. Ji, Y. Nishio, H. Lyu, J. B.-H. Tok and Z. Bao, *Science*, 2023, **380**, 735–742.
197 C. Wan, P. Cai, X. Guo, M. Wang, N. Matsuhisa, L. Yang, Z. Lv, Y. Luo, X. J. Loh and X. Chen, *Nat. Commun.*, 2020, **11**, 4602.
198 H. Tan, Y. Zhou, Q. Tao, J. Rosen and S. van Dijken, *Nat. Commun.*, 2021, **12**, 1120.
199 S. M. Won, H. Wang, B. H. Kim, K. Lee, H. Jang, K. Kwon, M. Han, K. E. Crawford, H. Li, Y. Lee, X. Yuan, S. B. Kim, Y. S. Oh, W. J. Jang, J. Y. Lee, S. Han, J. Kim, X. Wang, Z. Xie, Y. Zhang, Y. Huang and J. A. Rogers, *ACS Nano*, 2019, **13**, 10972–10979.
200 M. A. Lancaster, M. Renner, C.-A. Martin, D. Wenzel, L. S. Bicknell, M. E. Hurles, T. Homfray, J. M. Penninger, A. P. Jackson and J. A. Knoblich, *Nature*, 2013, **501**, 373–379.
201 X. Qian, H. N. Nguyen, M. M. Song, C. Hadiono, S. C. Ogden, C. Hammack, B. Yao, G. R. Hamersky, F. Jacob, C. Zhong, K. Yoon, W. Jeang, L. Lin, Y. Li, J. Thakor, D. A. Berg, C. Zhang, E. Kang, M. Chickering, D. Nauen, C.-Y. Ho, Z. Wen, K. M. Christian, P.-Y. Shi, B. J. Maher, H. Wu, P. Jin, H. Tang, H. Song and G. Ming, *Cell*, 2016, **165**, 1238–1254.
202 I. Chiaradia and M. A. Lancaster, *Nat. Neurosci.*, 2020, **23**, 1496–1508.
203 H. Cai, Z. Ao, C. Tian, Z. Wu, H. Liu, J. Tchieu, M. Gu, K. Mackie and F. Guo, *Nat. Electron.*, 2023, **6**, 1032–1039.
204 P. A. Merolla, J. V. Arthur, R. Alvarez-Icaza, A. S. Cassidy, J. Sawada, F. Akopyan, B. L. Jackson, N. Imam, C. Guo, Y. Nakamura, B. Brezzo, I. Vo, S. K. Esser, R. Appuswamy, B. Taba, A. Amir, M. D. Flickner, W. P. Risk, R. Manohar and D. S. Modha, *Science*, 2014, **345**, 668–673.
205 S. B. Furber, F. Galluppi, S. Temple and L. A. Plana, *Proc. IEEE*, 2014, **102**, 652–665.
206 A. Rao, P. Plank, A. Wild and W. Maass, *Nat. Mach. Intell.*, 2022, **4**, 467–479.
207 J. Yang, R. Wang, Y. Ren, J. Mao, Z. Wang, Y. Zhou and S. Han, *Adv. Mater.*, 2020, **32**, 2003610.
208 J. Göltz, L. Kriener, A. Baumbach, S. Billaudelle, O. Breitwieser, B. Cramer, D. Dold, A. F. Kungl, W. Senn, J. Schemmel, K. Meier and M. A. Petrovici, *Nat. Mach. Intell.*, 2021, **3**, 823–835.
209 W. Severa, C. M. Vineyard, R. Dellana, S. J. Verzi and J. B. Aimone, *Nat. Mach. Intell.*, 2019, **1**, 86–94.
210 B. V. Benjamin, P. Gao, E. McQuinn, S. Choudhary, A. R. Chandrasekaran, J.-M. Bussat, R. Alvarez-Icaza, J. V. Arthur, P. A. Merolla and K. Boahen, *Proc. IEEE*, 2014, **102**, 699–716.
211 M. A. Petrovici, B. Vogginger, P. Müller, O. Breitwieser, M. Lundqvist, L. Muller, M. Ehrlich, A. Destexhe, A. Lansner, R. Schüffny, J. Schemmel and K. Meier, *PLoS One*, 2014, **9**, e108590.
212 O. Richter, C. Wu, A. M. Whatley, G. Köstinger, C. Nielsen, N. Qiao and G. Indiveri, *Neuromorphic Comput. Eng.*, 2024, **4**, 014003.
213 C. Wang, X. Xu, X. Pi, M. D. Butala, W. Huang, L. Yin, W. Peng, M. Ali, S. C. Bodepudi, X. Qiao, Y. Xu, W. Sun and D. Yang, *Nat. Commun.*, 2022, **13**, 5216.
214 J. Wang, Q. Zhang, R. Chen, J. Li, J. Wang, G. Hu, M. Cui, X. Jiang, B. Song and Y. He, *Nano Today*, 2021, **41**, 101324.
215 L. Yang, H. Hu, A. Scholz, F. Feist, G. Cadilha Marques, S. Kraus, N. M. Bojanowski, E. Blasco, C. Barner-Kowollik, J. Aghassi-Hagmann and M. Wegener, *Nat. Commun.*, 2023, **14**, 1103.
216 Y. Wang, Y. Gong, S. Huang, X. Xing, Z. Lv, J. Wang, J.-Q. Yang, G. Zhang, Y. Zhou and S.-T. Han, *Nat. Commun.*, 2021, **12**, 5979.

217 S. Chen, Z. Lou, D. Chen and G. Shen, *Adv. Mater.*, 2018, **30**, 1705400.
218 Y. V. Pershin and M. Di Ventra, *Phys. Rev. E: Stat., Nonlinear, Soft Matter Phys.*, 2011, **84**, 046703.
219 G. Li, D. Xie, H. Zhong, Z. Zhang, X. Fu, Q. Zhou, Q. Li, H. Ni, J. Wang, E. Guo, M. He, C. Wang, G. Yang, K. Jin and C. Ge, *Nat. Commun.*, 2022, **13**, 1729.
220 W. Yi, K. K. Tsang, S. K. Lam, X. Bai, J. A. Crowell and E. A. Flores, *Nat. Commun.*, 2018, **9**, 4661.
221 R. Yuan, P. J. Tiw, L. Cai, Z. Yang, C. Liu, T. Zhang, C. Ge, R. Huang and Y. Yang, *Nat. Commun.*, 2023, **14**, 3695.
222 W. Wang, G. Pedretti, V. Milo, R. Carboni, A. Calderoni, N. Ramaswamy, A. S. Spinelli and D. Ielmini, *Sci. Adv.*, 2018, **4**, eaat4752.
223 C. Feng, B.-W. Li, Y. Dong, X.-D. Chen, Y. Zheng, Z.-H. Wang, H.-B. Lin, W. Jiang, S.-C. Zhang, C.-W. Zou, G.-C. Guo and F.-W. Sun, *Sci. Adv.*, 2023, **9**, eadg9376.
224 D. Farina, I. Vujaklija, M. Sartori, T. Kapelner, F. Negro, N. Jiang, K. Bergmeister, A. Andalib, J. Principe and O. C. Aszmann, *Nat. Biomed. Eng.*, 2017, **1**, 0025.
225 Y. H. Jung, B. Park, J. U. Kim and T. Kim, *Adv. Mater.*, 2019, **31**, 1803637.
226 X. Shi, H. Chen and X. Zhao, *Multimedia Tools Appl.*, 2021, **80**, 23297–23311.
227 W. Shi, Y. Guo and Y. Liu, *Adv. Mater.*, 2020, **32**, 1901493.
228 E. Dupont, J. Gomez and D. Bilodeau, *Int. J. Cosmet. Sci.*, 2013, **35**, 224–232.
229 G. P. Pfeifer and A. Besaratinia, *Photochem. Photobiol. Sci.*, 2012, **11**, 90–97.
230 D.-P. Häder, C. E. Williamson, S.-Å. Wängberg, M. Rautio, K. C. Rose, K. Gao, E. W. Helbling, R. P. Sinha and R. Worrest, *Photochem. Photobiol. Sci.*, 2014, **14**, 108–126.
231 H. Seung, C. Choi, D. C. Kim, J. S. Kim, J. H. Kim, J. Kim, S. I. Park, J. A. Lim, J. Yang, M. K. Choi, T. Hyeon and D.-H. Kim, *Sci. Adv.*, 2022, **8**, eabq3101.
232 S. L. Rumyantsev, S. Sawyer, M. S. Shur, N. Pala, Y. Bilenko, J. P. Zhang, X. Hu, A. Lunev, J. Deng and R. Gaska, *J. Appl. Phys.*, 2005, **97**, 123107.
233 M. P. Trawka, J. M. Smulko, L. Z. Hasse, C.-G. Granqvist, R. Ionescu, E. Llobet, F. E. Annanouch and L. B. Kish, *IEEE Sens. J.*, 2016, **16**, 5152–5159.
234 W. Li, F. Guo, H. Ling, P. Zhang, M. Yi, L. Wang, D. Wu, L. Xie and W. Huang, *Adv. Sci.*, 2017, **4**, 1700007.
235 J. Park, H. Seung, D. C. Kim, M. S. Kim and D. Kim, *Adv. Funct. Mater.*, 2021, **31**, 2009281.
236 G. J. Lee, C. Choi, D. Kim and Y. M. Song, *Adv. Funct. Mater.*, 2018, **28**, 1705202.
237 J. Wang, N. Ilyas, C. Li, K. Chen, D. Li, H. Zhao, D. Gu, F. Liu, Y. Jiang and W. Li, *Appl. Surf. Sci.*, 2023, **614**, 156232.
238 X. Ji, X. Zhao, M. C. Tan and R. Zhao, *Adv. Intell. Syst.*, 2019, **2**, 1900118.
239 J. A. Perge, K. Koch, R. Miller, P. Sterling and V. Balasubramanian, *J. Neurosci.*, 2009, **29**, 7917–7928.
240 M. Korte and D. Schmitz, *Physiol. Rev.*, 2016, **96**, 647–693.
241 J. Lisman, K. Cooper, M. Sehgal and A. J. Silva, *Nat. Neurosci.*, 2018, **21**, 309–314.
242 K. Mathieson, J. Loudin, G. Goetz, P. Huie, L. Wang, T. I. Kamins, L. Galambos, R. Smith, J. S. Harris, A. Sher and D. Palanker, *Nat. Photonics*, 2012, **6**, 391–397.
243 C. Hung, Y. Chiang, Y. Lin, Y. Chiu and W. Chen, *Adv. Sci.*, 2021, **8**, 2100742.
244 T. Ahmed, S. Kuriakose, E. L. H. Mayes, R. Ramanathan, V. Bansal, M. Bhaskaran, S. Sriram and S. Walia, *Small*, 2019, **15**, 1900966.
245 Y. Li, J. Wang, Q. Yang and G. Shen, *Adv. Sci.*, 2022, **9**, 2202123.
246 D. Li, C. Li, N. Ilyas, X. Jiang, F. Liu, D. Gu, M. Xu, Y. Jiang and W. Li, *Adv. Intell. Syst.*, 2020, **2**, 2000107.
247 C. Jo, J. Kim, J. Y. Kwak, S. M. Kwon, J. B. Park, J. Kim, G. Park, M. Kim, Y. Kim and S. K. Park, *Adv. Mater.*, 2022, **32**, 2108979.
248 Y. Hou, J. Li, J. Yoon, A. M. Knoepfel, D. Yang, L. Zheng, T. Ye, S. Ghosh, S. Priya and K. Wang, *Sci. Adv.*, 2023, **9**, eade2338.
249 Y. Zhou, I. Poli, D. Meggiolaro, F. De Angelis and A. Petrozza, *Nat. Rev. Mater.*, 2021, **6**, 986–1002.
250 Y. Zhou, Y. Jia, H. Fang, M. A. Loi, F. Xie, L. Gong, M. Qin, X. Lu, C. Wong and N. Zhao, *Adv. Funct. Mater.*, 2018, **28**, 1803130.
251 S. Hong, N. Zagni, S. Choo, N. Liu, S. Baek, A. Bala, H. Yoo, B. H. Kang, H. J. Kim, H. J. Yun, M. A. Alam and S. Kim, *Nat. Commun.*, 2021, **12**, 3559.
252 X. Yang, Z. Peng, H. Zuo, T. Shi and G. Liao, *Sens. Actuators, A*, 2011, **167**, 367–373.
253 F. Song, H. Su, J. Han, J. Xu and D. Zhang, *Sens. Actuators, B*, 2010, **145**, 39–45.
254 J. He, N. S. Villa, Z. Luo, S. An, Q. Shen, P. Tao, C. Song, J. Wu, T. Deng and W. Shang, *RSC Adv.*, 2018, **8**, 32395–32400.
255 R. A. Potyrailo, R. K. Bonam, J. G. Hartley, T. A. Starkey, P. Vukusic, M. Vasudev, T. Bunning, R. R. Naik, Z. Tang, M. A. Palacios, M. Larsen, L. A. Le Tarte, J. C. Grande, S. Zhong and T. Deng, *Nat. Commun.*, 2015, **6**, 7959.
256 C. Li, Y. Liu, W. Wan, Y. Li, Y. Ma, J. Zhang, X. Ren and H. Zhao, *Sens. Actuators, B*, 2020, **318**, 128209.
257 J. Zhang, Y. Liang, J. Mao, X. Yang, Z. Cui, S. Zhu and Z. Li, *Sens. Actuators, B*, 2016, **235**, 420–431.
258 R. S. Rao, B. Yadagiri, G. D. Sharma and S. P. Singh, *Chem. Commun.*, 2019, **55**, 12535–12538.
259 X. Wang, Q. Gao, M. Zhu, J. Wang, J. Zhu, H. Zhao, Z. L. Wang and T. Cheng, *Appl. Energy*, 2022, **323**, 119648.
260 R. Lei, H. Zhai, J. Nie, W. Zhong, Y. Bai, X. Liang, L. Xu, T. Jiang, X. Chen and Z. L. Wang, *Adv. Mater. Technol.*, 2019, **4**, 1800514.
261 J. Wang, C. Zhang, S. Gu, K. Yang, H. Li, Y. Lai and D. Yurchenko, *Aerosp. Sci. Technol.*, 2020, **103**, 105898.
262 N. R. Alluri, A. Chandrasekhar and S.-J. Kim, *ACS Sustainable Chem. Eng.*, 2018, **6**, 1919–1933.
263 R. L. Rutowski, *Sci. Am.*, 1998, **279**, 64–69.
264 S. D. Finkbeiner, A. D. Briscoe and R. D. Reed, *Evolution*, 2014, **68**, 3410–3420.

265 C. M. Nieberding, H. de Vos, M. V. Schneider, J.-M. Lassance, N. Estramil, J. Andersson, J. Bång, E. Hedenström, C. Löfstedt and P. M. Brakefield, *PLoS One*, 2008, **3**, e2751.
266 J. Andersson, A.-K. Borg-Karlson, N. Vongvanich and C. Wiklund, *J. Exp. Biol.*, 2007, **210**, 964–970.
267 A. D. Briscoe, A. Macias-Muñoz, K. M. Kozak, J. R. Walters, F. Yuan, G. A. Jamie, S. H. Martin, K. K. Dasmahapatra, L. C. Ferguson, J. Mallet, E. Jacquin-Joly and C. D. Jiggins, *PLoS Genet.*, 2013, **9**, e1003620.
268 K. Ozaki, M. Ryuda, A. Yamada, A. Utoguchi, H. Ishimoto, D. Calas, F. Marion-Poll, T. Tanimura and H. Yoshikawa, *Nat. Commun.*, 2011, **2**, 542.
269 Y. Zheng, S. Ghosh and S. Das, *Adv. Mater.*, 2024, **36**, 2307380.
270 Q. Xin, J. Zhang, Z. Han, H. Zhao, T. Hou, Y. Liu, S. Niu, Q. Han, Z. Mu, B. Li, Z. Wang and L. Ren, *Adv. Mater. Technol.*, 2023, **8**, 2200756.
271 R. R. Jackson and F. R. Cross, *Adv. Insect Physiol.*, 2011, **41**, 115–174.
272 M. E. Herberstein, A. E. Wignall, E. A. Hebets and J. M. Schneider, *Neurosci. Biobehav. Rev.*, 2014, **46**, 509–518.
273 F. G. Barth and P. Pickelmann, *J. Comp. Physiol. A*, 1975, **103**, 39–54.
274 E.-A. Seyfarth, *J. Comp. Physiol. A*, 1978, **125**, 45–57.
275 M. J. Harrington and P. Fratzl, *Prog. Mater. Sci.*, 2021, **120**, 100767.
276 A. Rising and M. J. Harrington, *Chem. Rev.*, 2023, **123**, 2155–2199.
277 A. Rising and J. Johansson, *Nat. Chem. Biol.*, 2015, **11**, 309–315.
278 W. Zhao, F. Shao, F. Sun, Z. Su, S. Liu, T. Zhang, M. Zhu, Z. Liu and X. Zhou, *Adv. Mater.*, 2023, **35**, 2300876.
279 M. Egmont-Petersen, D. de Ridder and H. Handels, *Pattern Recogn.*, 2002, **35**, 2279–2301.
280 B. Yegnanarayana, *Sadhana*, 1994, **19**, 189–238.
281 T. D. Albright, T. M. Jessell, E. R. Kandel and M. I. Posner, *Neuron*, 2000, **25**, S1–S55.
282 S. Dutta, M. Singh and A. Kumar, *Biomed. Signal Process. Control*, 2018, **39**, 378–389.
283 M. Zhou, H. Liu and Y. Hu, *Expert Syst.*, 2022, **9**, 39.
284 S. Mezzah and A. Tari, *Intell. Syst. Appl.*, 2023, **18**, 200212.
285 J. H. Viles, *Angew. Chem.*, 2023, **62**, e202215785.
286 W. Wei and X. Wang, *Aggregate*, 2023, **4**, e302.